Advanced Engineering Materials, Volume 26, Issue 6, March 2024, Article number 2301650
DOI: 10.1002/adem.202301650

A Review on Vibration Characteristics of Additively Manufactured Metal Alloys

Kashif Azher[1,2,†], Mussadiq Shah[1,2,†,], Ahmad Reshad Bakhtari[1,2], Gustavo M Castelluccio[3], Celal Sami Tüfekci[4], Andrea Cini[5], Nizami Akturk[1,2], Metin U Salamci[1,2,4]*

[1]Additive Manufacturing Technologies Application and Research Center, Ankara, Türkiye
[2]Department of Mechanical Engineering, Faculty of Engineering, Gazi University, Ankara, Türkiye
[3]School of Aerospace, Transport and Manufacturing, Cranfield University, Bedfordshire, UK
[4]Advanced Manufacturing Technologies Center of Excellence-URTEMM, Ankara, Türkiye
[5]Aerospace Engineering Department, University Carlos III of Madrid, Av. de la Universidad, 30, 28911, Leganes, Madrid, Spain
[*] E-mail: mussadiq.shah@gazi.edu.tr
[†] Equal contribution

Keywords: additive manufacturing, vibration, frequency, process parameters, orientation, geometry, modal analysis

The advent of additive manufacturing (AM) has dramatically shifted the manufacturing sector conceptualization, design, and creation of products. AM is poised to revolutionize goods production by establishing a new manufacturing paradigm, from reducing lead times to enabling rapid prototyping. AM can facilitate the production of complicated geometries and create functioning components with distinctive features for aerospace and automotive applications. However, defects such as pores, voids, interfaces, and inclusions can impair the quality and functionality of AM components.

Vibration Analysis (VA) has become a popular tool for the dynamic qualification and testing of products and non-destructive testing, but the literature lacks a comprehensive review of VA applied to AM. Hence, this paper summarizes recent advances in the application of VA for identifying and characterizing flaws in metal alloys, including titanium, aluminum, and nickel-based alloys produced by AM. The review also includes studies on defects, such as porosity, cracks, and inclusions, and their effect on VA. The article concludes with a discussion of the limitations of VA for defect characterization and future research directions. Overall, VA is a promising non-destructive testing

method for quality assurance in AM and offers insights on overcoming the difficulties for further development and application of this technology.

Nomenclature

AM	Additive Manufacturing
LPBF	Laser Powder Bed Fusion
SLM	Selective Laser Melting
EBM	Electron Beam Melting
PSP	Process Property Relationship
FGM	Functionally Graded Materials
E	Young's Modulus
ρ	Density
ω_n	Natural Frequency
FFT	Fast Fourier Transform
TPMS	Triply Periodic Minimum Surfaces
SR	Stress Relief
W-SR	Wrought Stress Relief
C	Damping Coefficient
SDC	Specific Damping Capacity
L-PBF	Laser Powder Bed Fusion

1. Introduction

Additive Manufacturing (AM), often referred to as 3D printing, has revolutionized the landscape of component design, manufacturing, and assembly in a multitude of sectors, ranging from biomedical and nuclear to transportation. Unlike traditional manufacturing methods, AM transcends the confines of conventional processes, offering unparalleled potential for complexity and customization.[1] This transformative technology enables the creation of intricately detailed structures previously inconceivable through traditional means.[2]-[5] AM can effectively fabricate components made of metal alloys using various techniques, [6] such as selective laser sintering, selective laser melting (SLM), and laser melting deposition.[7]-[14]

Laser-based techniques comprise numerous process attributes such as hatch spacing, laser power, scan speed, spot size,[15–19] deposition orientation,[15][20–23] or geometry.[24] These attributes, along with the scanning strategy and component shape, affect thermal history and determine the mechanical properties of the as-built parts.[25],[26] As the demand for advanced manufacturing solutions continues to surge, fully harnessing the potential of AM hinges upon a comprehensive

understanding of its behavior and properties under service conditions, such as dynamic loading from high-frequency vibrations to extreme temperatures. While traditional manufacturing methods have well-established prognosis principles, AM introduces additional complexities due to its layer-by-layer fabrication process and the inherent interaction of various process parameters. This complexity extends to understanding how these parameters influence the as-built part microstructure, thermal behavior, and mechanical performance.

Vibration analysis (VA) stands out as a potent and practical technique in the realm of dynamic behavior characterization for both materials and structures.[27,28] This methodology empowers engineers to identify potential failure modes and anticipate the response of components to external mechanical stimuli. The analysis of natural frequencies and mode shapes is a critical tool for robust component qualification and certification by detecting defects or anomalies in additively manufactured parts. The analyses of vibration signal deviations from nominal responses can identify the presence of cracks, voids, or delamination whereas real-time vibration monitoring during manufacturing can detect defects in production. [29] In addition, the VA can aid in evaluating the design of parts by analyzing their vibration responses and designing heterogeneous components to optimize their performance and reliability.[30] One such component design could be the lattice structure, which possesses excellent energy absorption and acoustic damping characteristics. Biocompatible Ti6Al4V metallic foams produced by AM are shown to have frequencies above the critical frequency compared to other metallic foams. [31] In addition, the porous layer achieved by lattice design provides an effective interaction and bonding with micro-perforated panels for outstanding performance. [32]

The metal alloys fabricated through the AM possess various types of defects. As the VA mainly uses the density and young's modulus values of the AM metal alloys, the porosity and cracking through the surface can be more susceptible to failure of AM parts by vibrations[33][34]. Similarly, because of process parameters, there are various defects like lack of fusion, [35] balling, [36] and keyhole depression, [37] which can also contribute to the changes in the mechanical properties of AM parts. [34] The defect mainly affects the tensile properties and density of the AM metal alloys; the more the porosity of the AM metal alloys, the more the density will reduce, which can change the natural frequencies of the AM parts. [38]

Significant progress has been made in exploring the realm of VA for polymers and their composite counterparts fabricated with AM. However, a relatively sparse body of work has concentrated on unraveling the vibrational behavior exhibited by AM-fabricated components crafted from pure metals and metallic alloys. This notable gap in the existing literature underscores a unique opportunity to probe the dynamics of this subset of materials.[39–44] The challenge lies in the

distinctive properties of metals and their alloys. Metals boast intrinsic characteristics that are inherently intertwined with their crystalline microstructures and complex interatomic interactions. This nuanced interplay, coupled with the intricate lattice configurations found within metals, potentially introduces a rich tapestry of vibrational behavior that merits exploration.

This article offers a thorough overview of the VA of AM metal alloys. By delving into a comprehensive synthesis of prior research endeavors, this article aims to shed light on the distinctive vibration behavior exhibited by AM metal alloys when juxtaposed against conventionally produced materials. A central focus of this article is to expound upon the vibrational characteristics manifested by AM materials, considering a diverse spectrum of influencing factors. Thus, it examines how varying process parameters, part orientation during the printing process, intricate geometries, and particle-damping effects collectively contribute to the vibrational attributes of AM-fabricated components. The article also discusses potential challenges and opportunities for future research, along with case studies that illustrate the use of VA methods on AM materials. By better understanding the response of AM materials to vibrational excitation, researchers can develop improved design guidelines and enhance dynamic loads functionality and characteristics of AM components.

2. Origin of materials effect on vibration analysis

Frequency analysis is often used to assess natural frequencies and associated vibration modes, which normally assumes a structural linear response under harmonic loads.[43] The analysis requires solving the structure dynamic equation to calculate the frequency or amplitude of the structure response as a function of frequency. Frequency analysis is often used in designing structures, including buildings, bridges, and machinery, to ensure that their natural frequencies do not coincide with the frequencies of anticipated loads, which might lead to resonance and potentially catastrophic collapse. [45,46] Several authors have recently investigated the dynamic properties of different materials and structures using model analysis.[47–53] Engineers can discover possible failure modes and enhance the structure design using modal analysis to determine the main vibrational modes of a structure. [27,54] However, sub and super-harmonics of these natural frequencies do not exhibit themselves in the modal analysis technique because of the assumption of linearity, which is the method's main drawback.

Structural dynamic analysis is a broader term used in various techniques for examining structural behavior under dynamic loads. Other methods like time-domain and response spectrum analysis also incorporate frequency and modal analysis. Compared to conventional materials, the anisotropic nature of AM materials leads to different dynamic behaviors, which require additional

considerations for predicting their properties. [11] For example, porosity and other microstructure defects can affect the vibrational behavior of the materials.[55]

Lattice morphologies and other complex geometric structures can significantly change the vibrational or damping characteristics of the materials. For example, Ti6Al4V, [24][56] stainless steel 316,[57] and other biocompatible materials with novel lattice structures can be fabricated with Electron Beam Melting (EBM) to develop implants for the biomedical industry. [58–60] Similarly, Functionally Graded Materials (FGM) are widely used for various applications, and various studies investigate their distinctive vibrational response. [55][61–64]

The dynamic behavior of materials and structures is often assessed by measuring the system reaction to a known input or excitation—typically mechanical vibration or shock. Critical information about a material or structure's properties, such as its natural frequency, damping, stiffness, and mode shapes, can be estimated.[65] Vibration analysis is particularly useful for assessing materials and structures subjected to cyclic or dynamic loads, such as those found in rotating equipment or vibrating structures. Engineers can identify and diagnose possible problems before they result in catastrophic failures by examining the vibration response of these systems. Vibration analysis may also be used to test the efficacy of design adjustments or revisions and to gauge how well the new materials or constructions will perform in actual usage.

The equation of a cantilever uniform beam in transverse vibration is determined using the static equilibrium equations by adding the forces and moments acting on the beam, following the Euler-Bernoulli beam theory. The free transverse vibration of a beam can be described by, [66,67]

$$\mathrm{EI}\frac{\partial^4 \mathrm{U}(x,t)}{\partial t^4} + \rho \mathrm{A}\frac{\partial^2 \mathrm{U}(x,t)}{\partial t^2} = 0 \qquad (1)$$

where E is the Young's modulus of the material, I is the second moment of inertia, ρ is Density, A is the cross-section area of the beam, and $U(x,t)$ is the beam transverse deflection.

$$\beta^4 = \frac{\rho \mathrm{A}\omega_{\mathrm{n}}{}^2}{\mathrm{EI}} \qquad (2)$$

and β corresponds to the dimensional frequency constant depending upon the type of the beam and ω_{n} is the natural frequency. From equation 2, we can separate the natural frequency, which would be equal to:

$$\omega_n = \beta^2 \sqrt{\frac{EI}{\rho A}} \qquad (3)$$

AM process parameters and manufacturing route can affect Young's modulus and Density, both of which inform the vibrational response. Hence, as per Equation 3, natural frequency and modal analysis require understanding the relationships between E and ρ with AM process parameters and

structures. The geometrical shape of the product is also a crucial parameter in VA that needs to be considered. The scope of VA can be expanded to encompass structures with diverse boundary conditions, geometries, and densities. Despite variations in these aspects, the fundamental definition remains consistent, as every structure possesses a specific boundary condition that can be approximated as a beam. This approach is mirrored in numerous existing studies. [67–70]

3. Effect of Process Parameters on Vibrational Characteristics of AM Materials

Among various AM process parameters, laser power, scan strategy, scan speed, spot size, build orientation, and hatch space significantly affects the mechanical response of the materials due to differences in residual stresses, influencing the Young's Modulus.[16,19,71] **Figure 1** shows the fundamental AM process parameters used to print parts. The melt pool shape, affecting the process stability and the quality of the finished component, is greatly influenced by the heat input governed by the process parameters. The melt pool instability can cause defects such as balling, and lack of fusion occurs due to insufficient laser power input or high scanning speed.[72,73] On the other hand, excess laser power input or low scanning speed can trigger the switching of laser melting mode from conduction to keyhole mode, making the melt pool deeper and creating keyhole porosities in the form of spherical gaps in the bottom of the melt pool.[74,75] The printing orientation can influence the vibration characteristics of a material in AM.[22,23,76] For instance, Lesage et al. analyzed the vibrational response of AlSi10Mg samples produced using conventional and AM methods.[21] The AM samples were printed in horizontal (flat), vertical (upright), and rotated orientations, with the build angle ranging from 0 to 90°. A cantilever beam with accelerometer sensors was employed to record displacement and frequency to determine the natural frequency of the samples. The Fast Fourier Transform (FFT) analysis depicted in **Figure 2** reveals that the frequency of the first vibration mode remains nearly identical for all AM and subtractive samples. Utilized extensively in spectrum analysis, the Fast Fourier Transform (FFT) is a potent vibration signal processor that yields the signal's amplitude, frequency, and phase.[77] However, slight differences emerge in the second and third vibration modes, particularly for the horizontally printed AM sample at a 90° rotation.

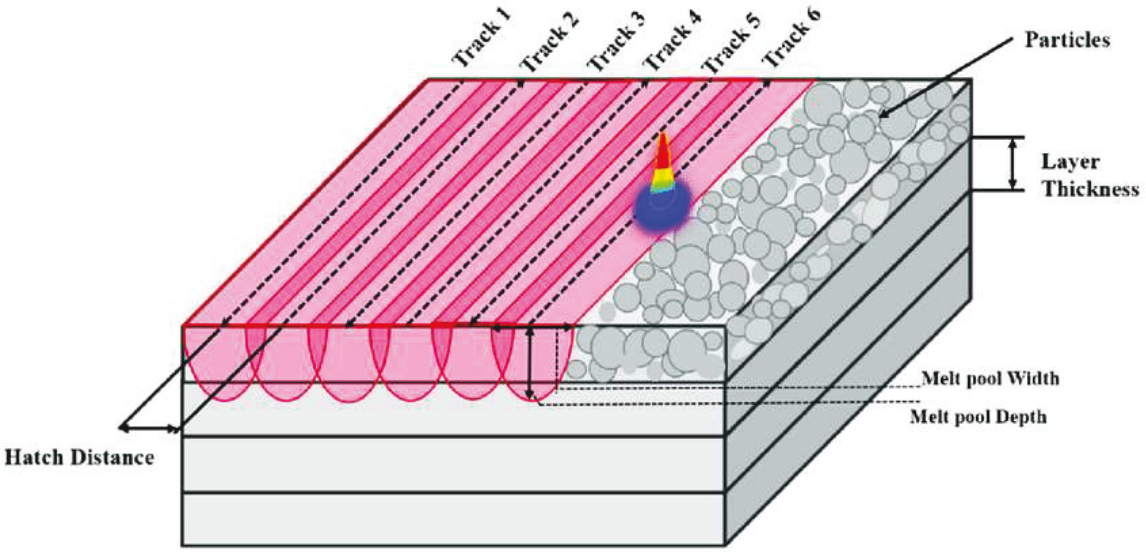

Figure 1. LPBF process parameters: laser power, scanning speed, hatch spacing, and layer thickness. (Reproduced under terms of the CC-BY license.[78] Copyright, 2023)

The presence of inhomogeneous material distribution along the sample gives rise to different dynamic responses, resulting in the horizontal sample being less stiff than the vertical and rotating orientations in printing. Stiffer samples exhibit higher natural frequencies, which explains why the vibration-damping characteristics of AM samples, in all orientations, are inferior compared to subtractive manufacturing.[79] The orientation in the SLM process differs for each sample, leading to an inhomogeneous distribution of material. As a result, the vibration-damping behavior of the samples also varies in response to random or sinusoidal inputs, affecting the propagation of waves.[80]

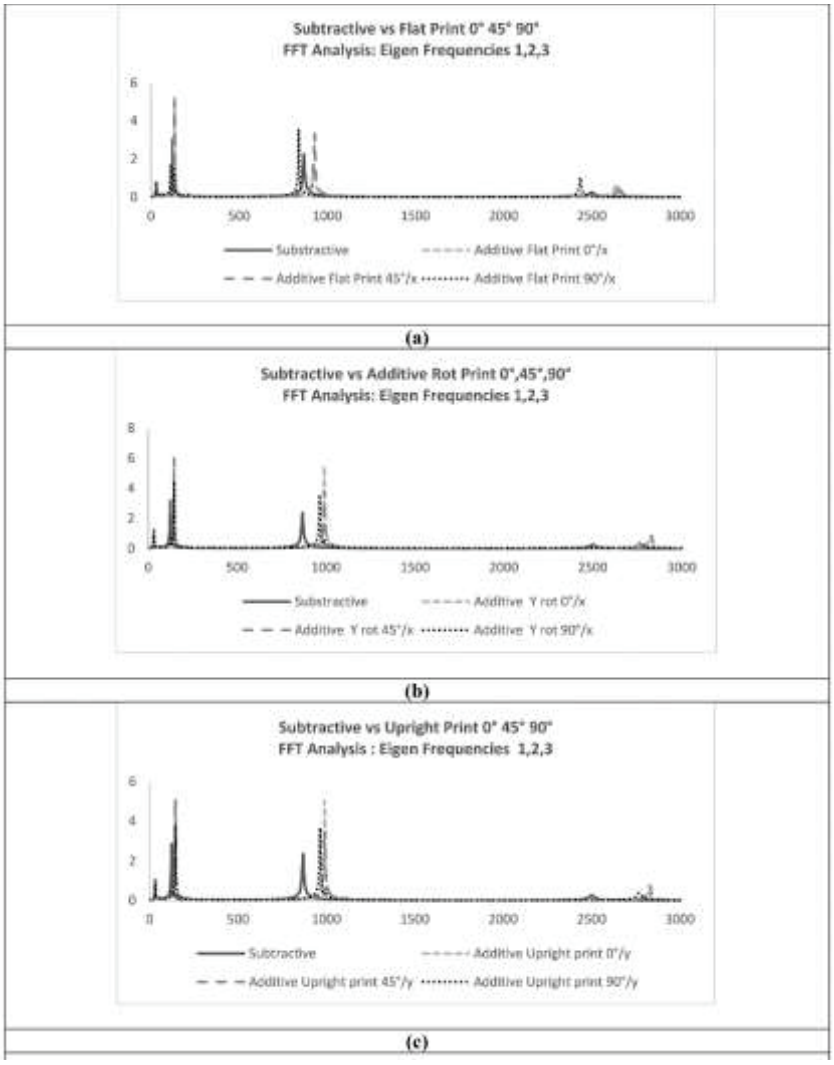

Figure 2. The Fast Fourier Transform (FFT) analysis observed for the subtractive and AM manufactured samples at 0°, 45°, and 90° for orientation of (a) Flat, (b) Rotation, and (c) Upright (Reproduced with permission from.[21] Copyright 2022, Elsevier)

Similarly, Ghadimi et al. studied the effects of printing orientation on AM samples and showed that vertical specimens exhibit low ductility due to more pores and defects than their horizontal counterparts.[23] A lower ductility usually correlates with lesser vibration-damping characteristics comparable to previous studies.[81–83] For instance, K. Guan et al. observed similar results for horizontal and vertical printed samples.[84] The latter behavior of AM components can also be explained based on the grain orientation during the solidification of molten metal. The AM building platform is parallel to the plane in which the molten layers are located. Therefore, the samples printed in different orientations had differing microstructures, resulting in varying material characteristics. Overall, these results from various efforts demonstrate that build orientation significantly affects the vibration characteristics and can be used to engineer the material properties by optimizing build orientations.

Kladovasilakis et al. studied the effect of varying laser power, scanning speed, and spot size on the Inconel 718 AM samples.[16] Based on the experimental results, a regression model relating Young's Modulus E with the processing parameters was developed, as shown in **Figure 3**. [16] The model shows that Young's modulus decreases as the scanning speed increases. Similarly, the study conducted by Valdez et al. also indicates that increasing the scanning speed contributes to a decrease in E and Density.[85] The effects of scanning speed on material vibration characteristics can be inferred through **Equation 3**.[17] It indicates that an increase in scanning speed generally leads to a decrease in the natural frequency.

Furthermore, increasing the spot size and laser power increases E to some extent. However, beyond a certain threshold, a further increase in spot size and laser power leads to a decrease in the value of E [16] The impact of power and spot size on the natural frequency can vary, potentially resulting in an increase or a decrease, such as in [85]; the authors reported that an increase in laser power led to a reduction in both E and Density, subsequently impacting the natural frequency. Similarly, variation in scanning strategy affects the vibrational characteristics of the AM parts. Cobbs et al. investigated the effect of five different scan strategies (i.e., continuous skywriting, continuous with no skywriting, strip skywriting, strip with no skywriting, and island strategy) on Inconel 718 AM samples [17] A continuous scan pattern without skywriting resulted in beams with the lowest densities and natural frequencies across all vibrational modes. In contrast, the island strategy produced test specimens with densities and vibrational modes resembling wrought Inconel 718. Additionally, the island strategy approach exhibited higher frequency among the built parts than other strategies. Interestingly, the vibrational modes of the continuous and strip scanning strategies did not show significant differences from each other. [17]

The scanning strategy is another important parameter that can impact the mechanical properties of the AM parts. It changes the heat input to the material, affecting the residual stress generation in the built parts. Studies have demonstrated that adopting an island scanning strategy in AM results in the lowest residual stress levels compared to other scanning strategies.[86] Reducing residual stress has a beneficial effect on the mechanical properties and vibrational characteristics of AM parts. Using the island scanning strategy helps to mitigate stress concentrations and potential distortions, improving structural integrity and stability. These factors contribute to enhanced vibrational behavior in the printed components. [17]

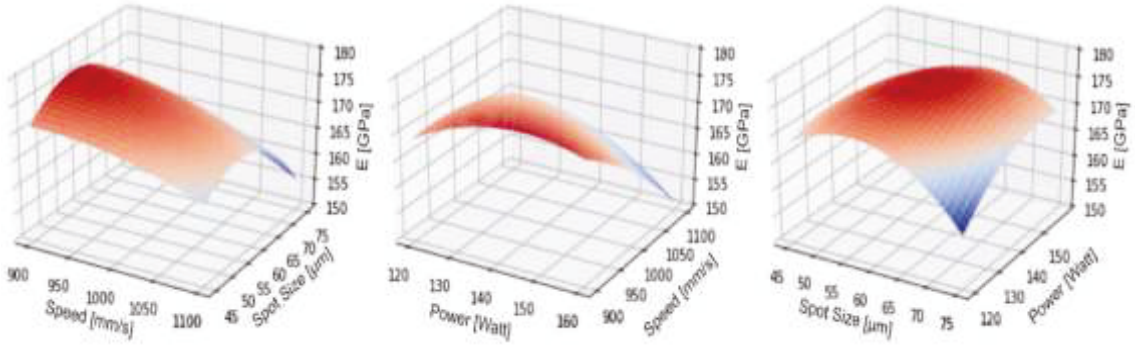

Figure 3. The regression model obtained from experimental data for E varying with scanning speed, spot size, and laser power Inconel 718 (Reproduced under terms of the CC-BY license [16], Copyright 2022)

Hatch spacing also contributes to the variation in Young's modulus and Density, affecting the vibrational characteristics of the AM parts. West et al. used hatch spaces between 75 – 150 µm on SS304 samples.[87] The samples were printed on a plate with a specific orientation to observe the natural frequency. **Figure 4** presents the Frequency Response Function (FRF) of the component, illustrating the three vibration modes and the plate resonance. FRF is the ratio at the applied frequency between the response and excitation of the system.[88] FRF represents three values that must be displayed: the complex function of the frequency and the real and imaginary components.[89] The results indicated that Density decreases with an increase in hatch spacing (**Figure 5(a)**). Besides, **Figure 5(d)** demonstrates that Young's modulus initially increases until a hatch spacing value of 105 µm and decreases afterward. Consequently, the variations in *E* and Density substantially impact the vibrational behavior. The frequency analysis for the first three vibration modes, shown in **Figure 5(g)**, represents a similar trend for *E* concerning hatch spacing. The frequency for all three modes initially increases till 105 µm and decreases afterward, attributed to the lack of fusion and porosity.[87] (**Figure 5(b),(c),(e),(f)**).

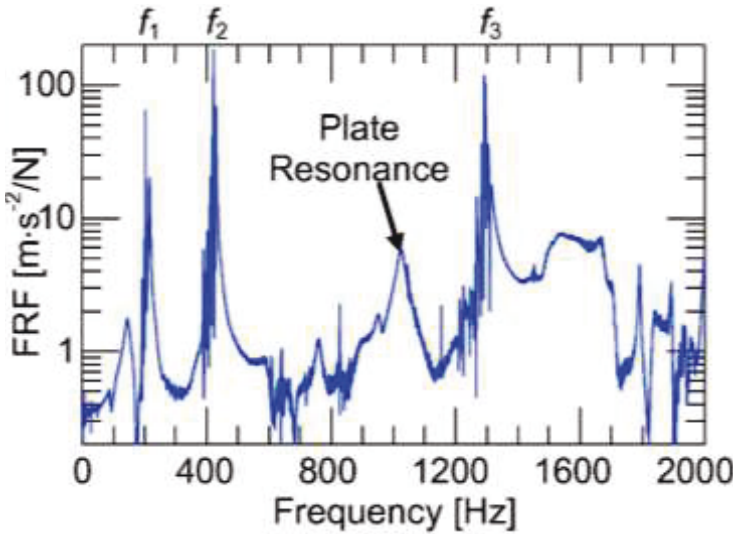

Figure 4. Experimental setup with samples and the samples' FRF graph with three modal frequencies (Reproduced with permission from. [87] Copyright 2017, Elsevier)

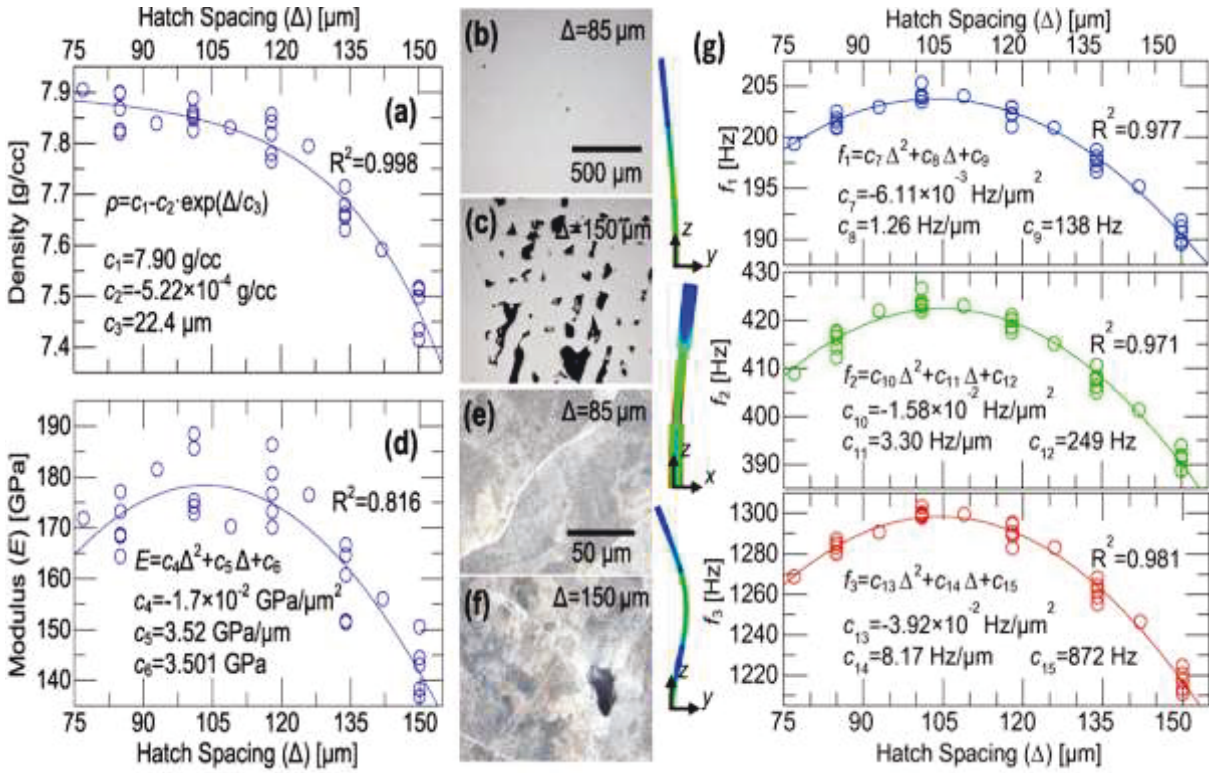

Figure 5. (a) shows the relation between hatch spacing and Density of the exponential behavior, (b),(c), (e), and (f) shows the micrographs at different hatch spacing, (d) shows the relationship between hatch spacing, and E shows a polynomial curve while (g) Relationship between the natural frequency of the first three modes and hatch spacing (Reproduced with permission from. [87] Copyright 2017, Elsevier)

These results demonstrate that the unique combination of process parameters employed in AM gives rise to a Volumetric Energy Density (VED) that significantly influences the mechanical behavior of materials, affecting the vibration response. A significant consensus exists within the literature about the VED as a highly effective parameter for defining the required energy needed to get dense components in Laser Powder Bed Fusion (LPBF) processes.[90] The primary purpose of utilizing the VED is to characterize the empirical observations obtained from LPBF experiments.[91][92] The formulation begins by considering the most crucial process parameters in the following manner:

$$VED = \frac{P}{Vht}$$

In particular, variations in the VED can lead to differences in the degree of fusion or the extent of melting during the AM process, thereby influencing the E value.[16][85][87] **Figure 6** presents data reported in the literature relating the VED to E. [16] The plotted data shows a non-linear relationship between them where at lower VEDs, the E values are higher, but as the VED increases, the E values fluctuate and make it very difficult to find the optimum range of VED for the desired E, as it is in the case of relative density.[93] In addition, the optimum range of required VED can vary from one material to another, and it needs to be considered while using the VED as a collective parameter for studying the mechanical properties of the as-built AM parts. Hence, only looking at the energy density arising from process parameters cannot be single-handedly effective in optimizing the E because it only considers the four process parameters (i.e., laser power, hatch space, scan speed, and layer thickness) and excludes other parameters and material properties affecting the E. Therefore, a comprehensive study would be needed considering the important processing parameters, material properties, and other factors affecting the E. One such solution could arise from the modification of the VED formula to include the mentioned aspects for optimizing the E. [92][94]

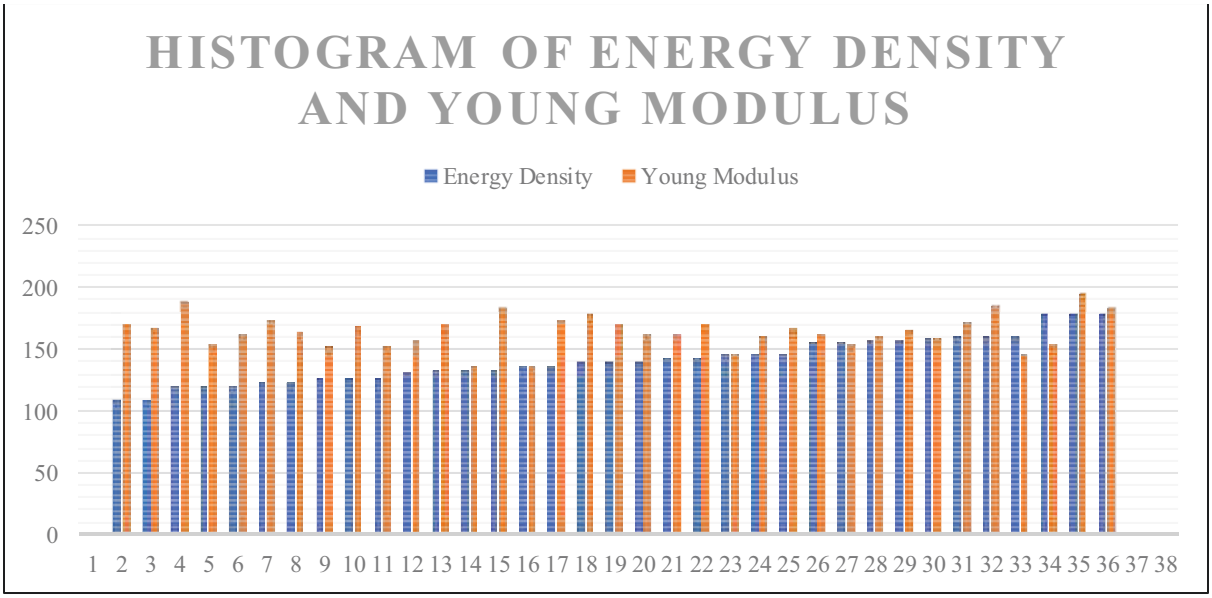

Figure 6. shows the relation between VED and *E* using the tabular data from the literature [16]

5. Effect of AM-fabricated geometries on vibrational characteristics

The vibrational characteristics of materials in AM vary depending on the geometry type and structural changes.[95] The geometry of AM-fabricated metal alloys significantly influences the vibrational and damping performance.[96,97] The AM technology helps to fabricate complex geometries, such as cellular or lattice structures (LSs). The LSs are naturally inspired structures formed by repeating the fundamental building block known as the unit cell.[98] The LSs have various applications and advantages as compared to conventional parts. The lattice structures vary the mechanical properties of the AM parts.[99] As discussed in the section related to VA, the vibration characteristics are mainly governed by Young's modulus and Density. Hence, changing the type of lattice structure would also affect the vibrational characteristics of AM lattice parts.[100] Moreover, the cell size with different unit cell thickness can also influence the elastic properties. The LSs make the ideal parts with the optimized property for strength-to-weight ratio. It will be beneficial to use LSs as a design for sustainability, as it will reduce energy consumption. The biomedical application for the LSs is widely utilized in literature, as the mechanical properties of the LSs can be matched with the specific requirements for the human bones.

LSs are used in various technical applications because they exhibit a high strength-to-weight ratio. Nowadays, improvements in AM have made it possible to manufacture complex lattice structures like triply periodic minimum surface (TPMS) models. Liu et al. studied Ti alloys, investigating the dynamic behavior of various lattice structures made of Ti-6Al-4V.[24] They examined three cell sizes and four different lattice structure types, as shown in **Figure 7. Figure 8 (a)** demonstrates the behavior of the printed cells. Cell 3, with a 1.2 mm size, exhibits the highest

natural frequency, comparable to that of a solid sample. The natural frequency and Density exhibit a similar trend for cells 2 and 3, while there is a slight variation for cells 1 and 4. As a result, it reinforces the observation that density variation due to different lattice types affects the overall vibrational behavior.

Furthermore, **Figure 8 (b)** presents the damping ratio of the four different cell types with varying cell sizes compared to solid samples. The damping ratio is generally defined as the measure of the energy dissipated by any system under vibrational loads or conditions. As the damping ratio increases, the amount of energy dissipated also increases, which helps reduce the effects of vibrations. For instance, if the damping ratio of the system is between zero and one, the system is underdamped, while for one, the system is critically damped. The value above one is usually defined as the overdamped system.[66][101] Among the cells, Cell 3, referred to as Solidify, exhibits the highest damping ratio, indicating good vibration-damping characteristics. Interestingly, there is an inverse relationship between the natural frequency and the damping ratio. Higher natural frequencies are associated with lower Density, which increases the specimens' stiffness and reduces their vibration-damping characteristics. The lattice or porous structures exhibit excellent vibration-damping characteristics compared to solid samples.

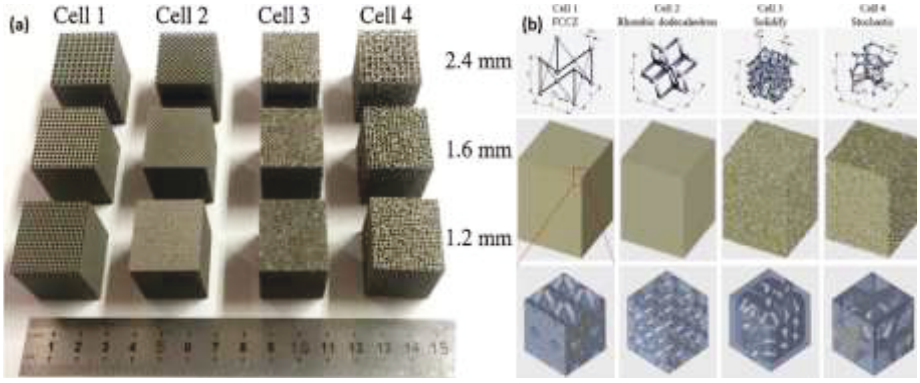

Figure 7. (a) Actual, and (b) schematic image of the cells and the lattice structures (Reproduced with permission from. [24] Copyright 2021, Elsevier)

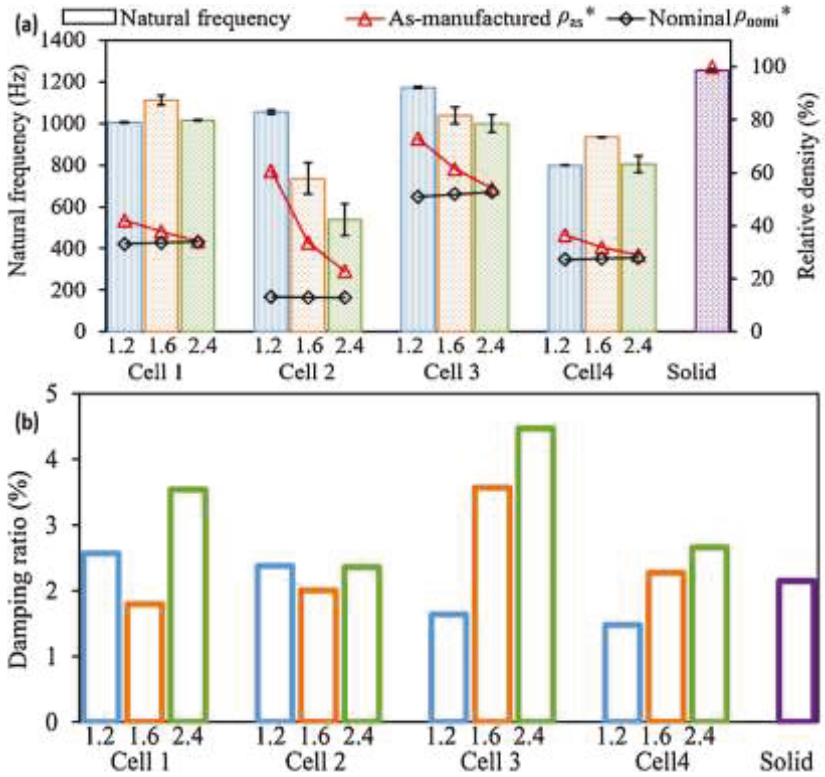

Figure 8. (a) The relationship between the natural frequency of Laser Powder Bed Fusion (L-PBF) build Ti6Al4V with varying cell types and sizes while comparing it to a solid sample (b) Relationship between the damping ratio of L-PBF build Ti6Al4V with varying cell types and sizes while comparing it to a solid sample (Reproduced with permission from. [24] Copyright 2021, Elsevier)

Ramadani et al. further investigated the vibration-damping efficiency of AM parts by incorporating a lattice structure using different materials.[56] Three gear geometries were studied, including solid gear and lattice structure gears, one filled with polymer. Figure 9 presents the frequency spectrum for each sample, where the solid gear exhibits the tallest and most distinct peaks. In contrast, the lattice structure gear reduced the maximum amplitude and distributed the amplitudes of significant harmonics more evenly. This effect was particularly pronounced in gear with polymer infill, as its vibration energy spectrum demonstrated a decrease in amplitudes. The findings highlight the effectiveness of a lattice body construction in minimizing gear vibrations. Moreover, it is suggested that implementing polymer enhances structural damping, providing valuable benefits. In another study, M. Kam et al. conducted experimental investigations into the damping properties of metal/polymer composite sleeve bearings.[102] They revealed that composite sleeve bearings, characterized by diverse constructions and varying occupancy rates, exhibited substantial disparities in their damping capacities. Among these variations, sleeve bearings featuring a 3D honeycomb filling structure demonstrated a notably heightened capacity for vibration absorption. This

observation implies that the intricate honeycomb-filling structure plays a pivotal role in enhancing a bearing's ability to attenuate vibrations, particularly concerning occupancy rate.

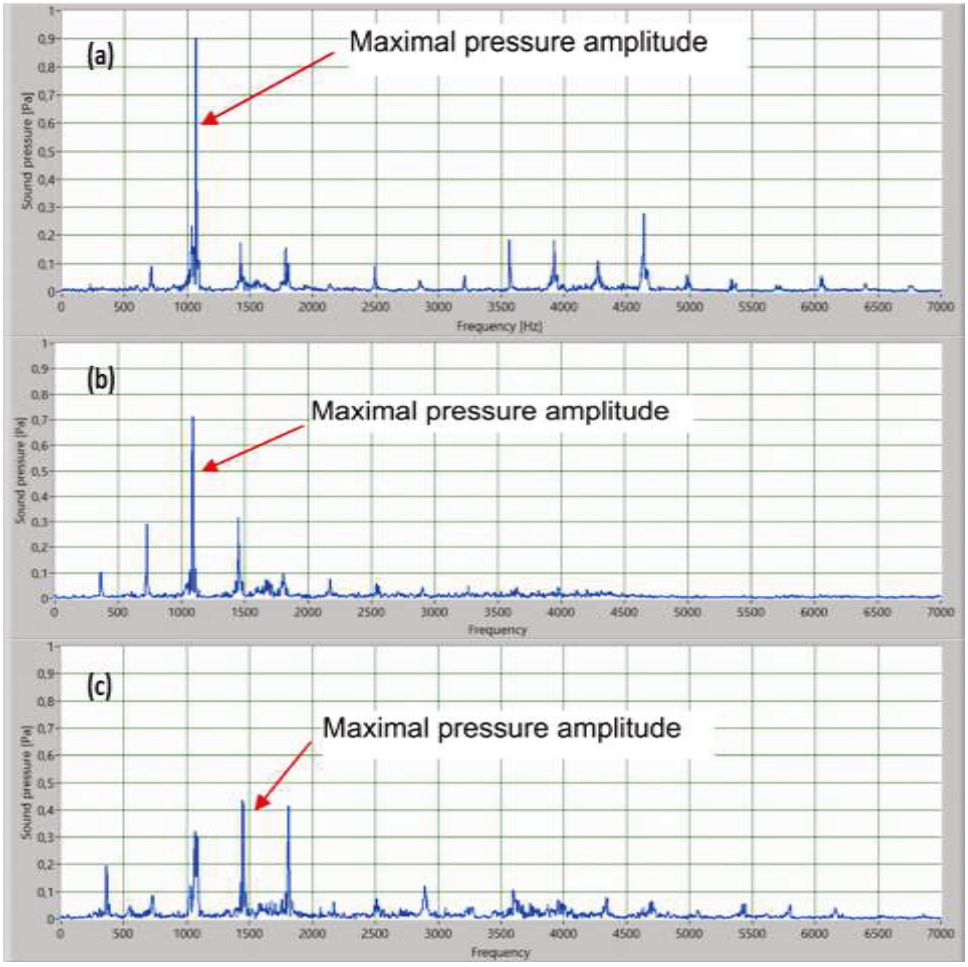

Figure 9. Frequency response of the sound pressure for gears having (a) solid body (b) lattice structure (c) lattice structure with polymer inserted (Reproduced with permission from. [56]Copyright 2021, Springer)

Hussain et al. examined the practical application of vibration analysis for AM parts incorporating lattice structures within airfoils.[103] The authors specifically investigated the comparison between a solid blade model and a model with a lattice structure inside the blades, utilizing the NACA 23012 standard airfoil profile. As presented in **Figure 10** and Table 1 the frequency results reveal that the lattice blades exhibit higher natural frequencies for the first and third modes than the solid blades. Notably, the solid blade model demonstrates a minimum natural frequency of 1887.50 Hz and a maximum natural frequency of 1987.50 Hz for the 0.25 mm lattice blade model. Furthermore, a decrease in lattice unit cell thickness corresponded to an increase in the first and third natural frequencies. Modal analysis findings indicate that lattice-based blades generally exhibit higher natural frequencies. In turbine applications, the working speed of stiff rotors needs to be lower than the first natural frequency, making an increase in the first natural frequency desirable.

For instance, Presas et al. suggest that raising the natural frequency can extend the operating speed range of turbines.[104] Since the natural frequencies in the second and third modes surpassed the average turbine operating speed, they were not considered significant.

Table 1. Experimental modal natural frequencies for solid and lattice-type blades (Table Reproduced under terms of the CC-BY license [103])

Number of modes	Lattice Blade with 0.25 mm thickness	Lattice Blade with 0.5 mm thickness	Lattice Blade with 0.75 mm thickness	Solid Blade Model
First	1987.50	1962.50	1925.00	1887.50
Second	4650.00	4675.00	4700.00	4762.50
Third	5950.00	5900.00	5850.50	5837.50

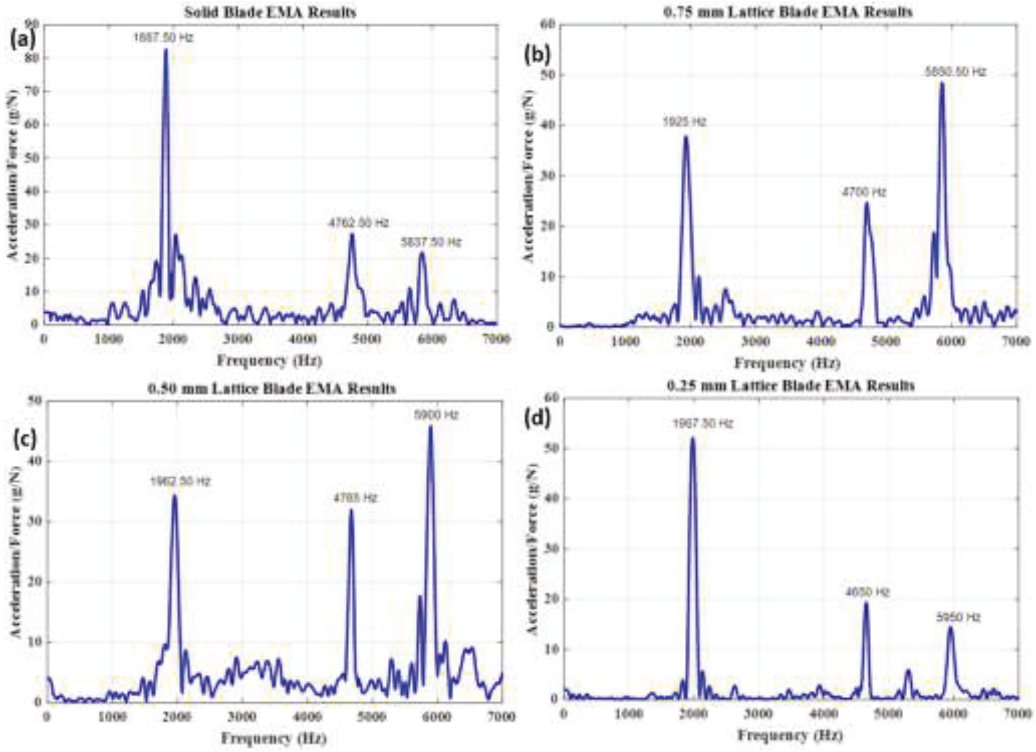

Figure 10. FRF of experimental three modes of vibration for (a) solid and lattice thicknesses of (b) 0.75 mm, (c) 0.5 mm, and (d) 0.25mm for blades (Reproduced under terms of the CC-BY license [103] Copyright 2022)

The damping ratio presented in Table 2 indicates that the first mode exhibits the highest damping ratio. Unlike solid blade models, the lattice models show a slightly higher damping ratio in the first modal vibration. The first mode consistently demonstrates the highest damping for all blade models, with the 0.75 mm lattice blade model exhibiting the maximum value of 0.0251. The results align with the preference for high damping ratios, effectively absorbing vibration energy, reducing vibratory stresses, and ultimately enhancing turbine blade lifetime.[103] Additionally, the variation in lattice structure thickness contributed to improved vibration damping, as evident in Error! Reference

source not found. when comparing the damping ratios, which is consistent with the findings of Liu et al.

Moreover, simulation results indicated that the initial mode for all blade types is the flap-wise bending mode. In this mode, the solid blade model demonstrated the lowest natural frequency of 1813.10 Hz, while the 0.25 mm lattice blade model exhibited the highest natural frequency of 1971.40 Hz. The lattice blade shows an approximately 8% higher natural frequency than the solid blade in the flap-wise bending mode. The trend is inverted for the second and torsional modes, where the solid blade has the highest natural frequency. The torsional mode is also observed in the third mode, with the 0.25 mm lattice blade exhibiting the highest natural frequency.

Table 2. Damping ratio of solid and lattice structured blades estimated from experimental results (Table Reproduced under terms of the CC-BY license [103])

Number of modes	Lattice Blade with 0.25 mm thickness	Lattice Blade with 0.5 mm thickness	Lattice Blade with 0.75 mm thickness	Solid Blade Model
First	0.0244	0.0220	0.0251	0.0212
Second	0.0070	0.0071	0.0089	0.0070
Third	0.0073	0.0073	0.0066	0.0079

Similarly, Simsek et al. analyzed the modal characterization of TPMS AM structures using HS188 alloy.[105] The study involved four TPMS structures: primitive (P), Gyroid (G), diamond (D), and Schoen IWP, as depicted in **Figure 11.** For frequencies up to 7100 Hz, the FRF shown in **Figure 12 (a)** exhibited similar behavior. However, beyond this frequency limit, changes in the frequencies were observed. Specifically, the diamond structure exhibited the lowest value (10710 Hz), while the primitive structure demonstrated the highest value (11600 Hz) in the third mode. The findings highlight the influence of lattice structures on material behavior and demonstrate that altering the structures is relatively feasible using AM techniques. [105]

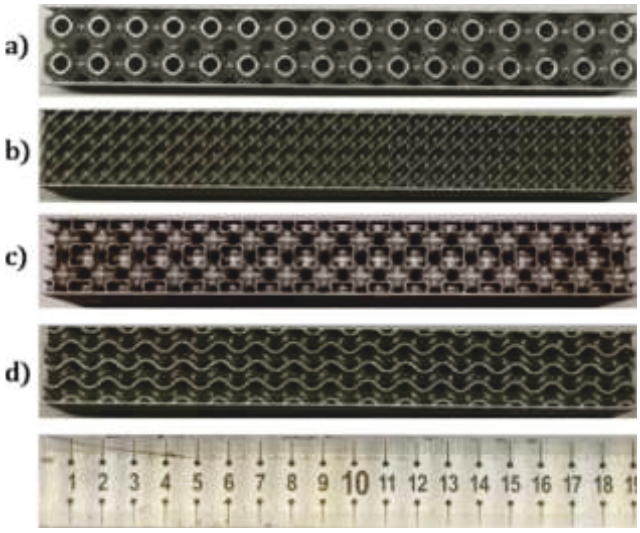

Figure 11. Experimental samples with lattice structures of (a) primitive (b) diamond (c) IWP (d) gyroid (Reproduced with permission from. [105] Copyright 2021, Springer)

In **Figure 12 (b) to (g),** the frequencies of TPMS structures are compared while varying the relative Density from 0.1 to 0.5. Modal analysis was conducted for each TPMS structure to investigate the results for the bending, torsional, and longitudinal modes. All TPMS structures exhibited a linear relationship with the volume fraction, with the bending mode displaying greater sensitivity to changes in volume fraction. The change in frequency for TPMS structures was substantial in the bending mode (2.5 times) compared to the torsion mode (0.4 times) when altering the volume fraction. Concerning the bending mode, the primitive, IWP, and Gyroid structures showed greater sensitivity to changes in volume fraction, while the diamond structure was the least affected in all three modes: bending, torsion, and longitudinal. A consistent pattern can be observed across the first three bending modes for all TPMS structures. The highest modal frequency at a relative density of 0.5 was observed for the IWP structures, even though the diamond structure exhibited the highest modal frequency at a relative density of 0.1. The same bending mode is evident in diamond and IWP-type cell structures at a relative density of 0.3. The comparison between the Gyroid and primitive structures yielded similar results.

Regarding torsion modes 1 and 2, the primitive structure demonstrated the best torsional properties, followed by the Gyroid, diamond, and IWP structures. The diamond and Gyroid structures performed similarly in torsion modes. The longitudinal mode exhibited the same trend as the bending modes for the TPMS structures. The diamond structure exhibited the highest longitudinal modal frequency at a relative density of 0.1. However, at a relative density of 0.5, the IWP structure exhibited the highest longitudinal modal frequency.

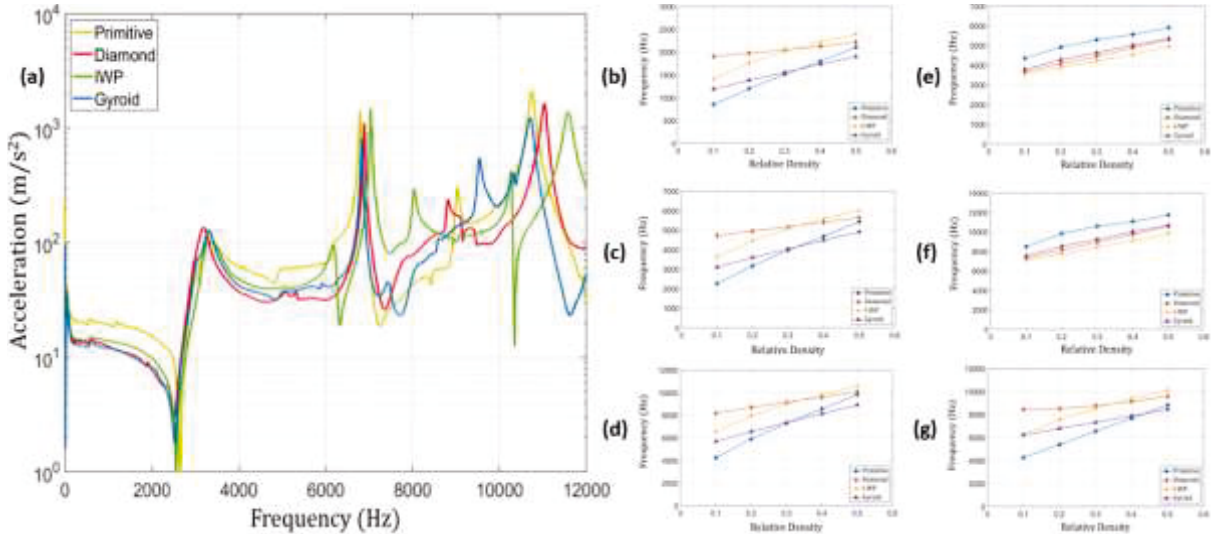

Figure 12. (a) FRF response of the primitive, diamond, IWP, and gyroid lattice structures Experimental modal analysis for lattice structures at (b) first, (c) second, and (d) third bending modes, (e) first and (f) second torsion modes, and (g) longitudinal mode (Reproduced with permission from. [105] Copyright 2021, Springer)

Considering aerospace applications, Bari and Bollenbach proposed replacing the motor holder's regular geometry with lattice structures, as shown in **Figure 13**.[106] The material used in the motor holder is Aluminium 6061T. Although the study comprises only simulations, results significantly differ from the solid holder, which is helpful for future studies.

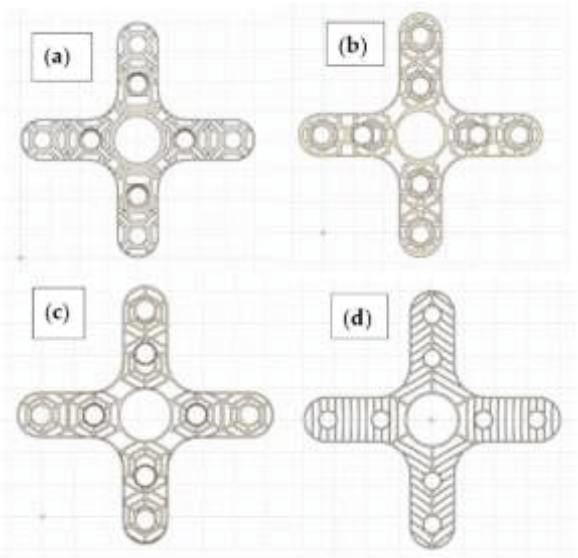

Figure 13. Lattice structures used for a motor holder, namely (a) polyhedral, (b) snowflake, (c) circular, and (d) linear spider web (Reproduced under terms of the CC-BY license. [106] Copyright 2022)

The results of the modal frequency analysis simulation reveal that the motor holder with linear spider-web unit cells exhibits the most significant reduction in noise vibration compared to mode

frequency (1), as presented in Table 3**.** This design demonstrates high resilience to vibration in aircraft applications, which is particularly important in aeronautical, where weight reduction is crucial. Among the different modes, mode (1) possesses the lowest frequency while maintaining an adequate level of safety. The linear spider-web motor holder, weighing only 0.3473 g with a porosity of 84%, offers the lightest weight. By fulfilling the required standards, the linear spider-web holder demonstrates strong mechanical properties while minimizing weight. Various factors influence the holder's mechanical properties, including design, porosity, and material selection. The primary objective of this project was to develop a design concept for brushless motors that achieves weight and noise reduction, regardless of whether the item is manufactured using SLM. [106]

Table 3. Modal natural frequencies simulation results (Table Reproduced under terms of the CC-BY license [106])

Number of modes	Lattice Blade with 0.25 mm thickness	Lattice Blade with 0.5 mm thickness	Lattice Blade with 0.75 mm thickness	Solid Blade Model	Holder without lattice
First	9766	11072	10530	9542	15351
Second	19081	17756	19762	12856	28315
Third	20078	21895	19907	17864	28343
Fourth	33069	21945	27846	20451	43761
Fifth	34996	26289	31404	21102	49730
Sixth	35249	28467	31478	23381	63426
Seventh	38256	30596	34528	24270	64649
Eighth	39823	30987	34605	24715	69107

Several approaches have been proposed to reduce vibration and improve damping, with conventional materials exhibiting different vibration behavior than AM materials. One critical issue discussed by Raval et al. is the vibration of AM materials during machining.[107] The study focused on the effect of cutting forces on Titanium alloy, considering four samples: Wrought (W), Wrought-Stress Relieved (W-SR), AM, and AM-SR. In general, titanium alloy is machined under wet conditions to prevent high temperatures during cutting, as temperature plays a crucial role in wear and vibrations. The cutting temperature of AM samples was lower than that of the wrought samples, with the AM-SR sample exhibiting the lowest cutting temperatures. These results align with the hardness values and specific cutting forces, indicating reduced heat and mechanical stresses during the cutting of AM components.

Figure 14 (a) and (b) demonstrate that both Titanium Wrought (W) and Wrought-Stress Relieved (W-SR) exhibit lower vibrations compared to the AM samples during cutting. However, if stress relief (SR) is applied to the AM samples, the vibration improves and becomes comparable to the wrought material. This improvement can be attributed to the microstructure created by the AM process. The wrought material has equiaxed grains, while the AM samples exhibit slender needle-

like grains. [107] Also, known defects in AM parts, such as pores, flaws, oxygen contamination, and inclusions, could contribute to the observed vibrations. **Figure 14 (c) and (d)** indicate that these vibrations do not follow a specific pattern, suggesting that the vibration source is the material rather than the machine tool. However, heat treatment, specifically in the case of AM-SR compared to AM without stress relief, appears to reduce the wide-band vibration observed in the printed components. AM-SR vibrations are comparable to those observed in the wrought material in frequency. [107]

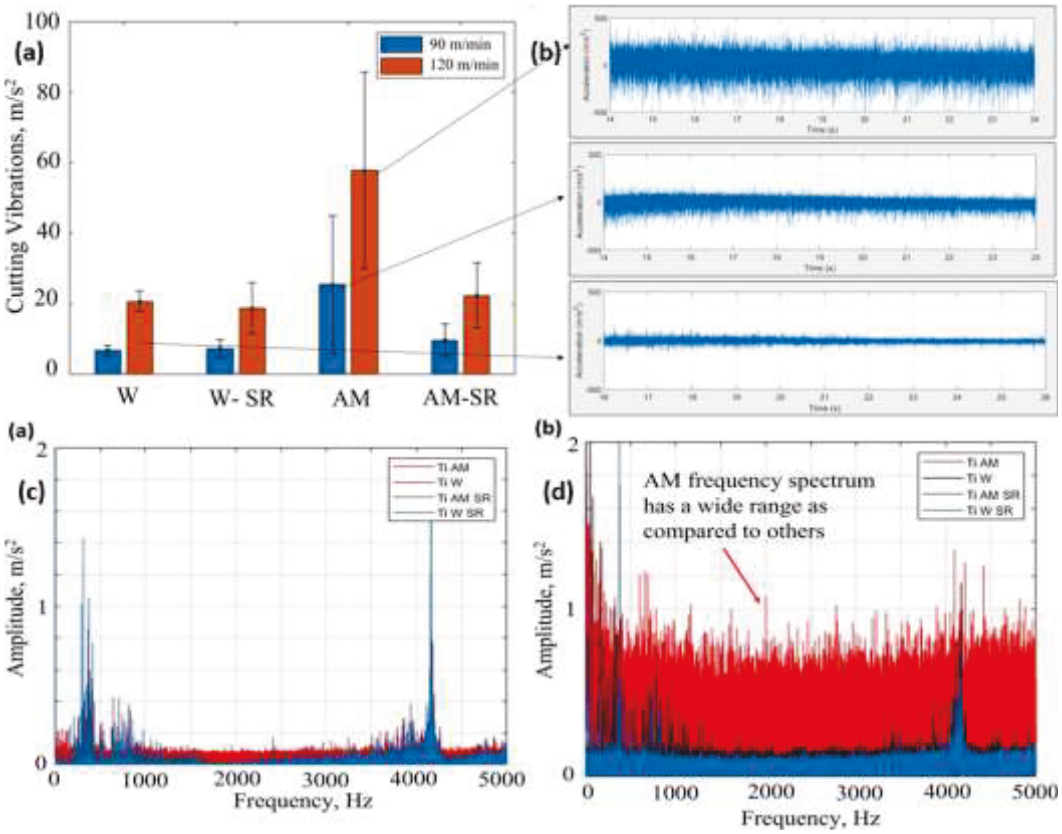

Figure 14. (a) Histogram of cutting vibrations, (b) vibration response for AM samples at cutting velocities of 120 m/min and 90 m/min and Wrought sample at 120 m/min. FFT analysis of cutting vibrations to compare AM and Wrought materials for cutting velocities at (c) 90 m/min and (d) 120 m/min (Reproduced with permission from. [107] Copyright 2023, Elsevier)

For observing the AM sample related to different vibrations, some studies have suggested using particle damping or inherent damping.[18][108–113] In their study, Ehlers et al. proposed using particle dampers for AM samples, as illustrated in **Figure 15 (a)**.[113] The concept of employing particle damping proved to be effective in reducing the vibrations of AM samples. **Figure 15 (b)** demonstrates the distinct differences in FRF among fully fused beams, fused beams with cavities, and particle-damped beams. The particle-filled beam exhibits the lowest amplitude and maximum damping, indicating its superior vibration reduction capabilities. The natural frequency of the particle-filled beam closely matches that of the hollow unfilled beam, suggesting that the particles have a

minimal impact on frequency shift but contribute to non-linear damping. Moreover, the fully fused beam and the partially filled beam with cavities exhibit damping values of a similar magnitude, enabling accurate quantification of the influence of particle damping on a beam.

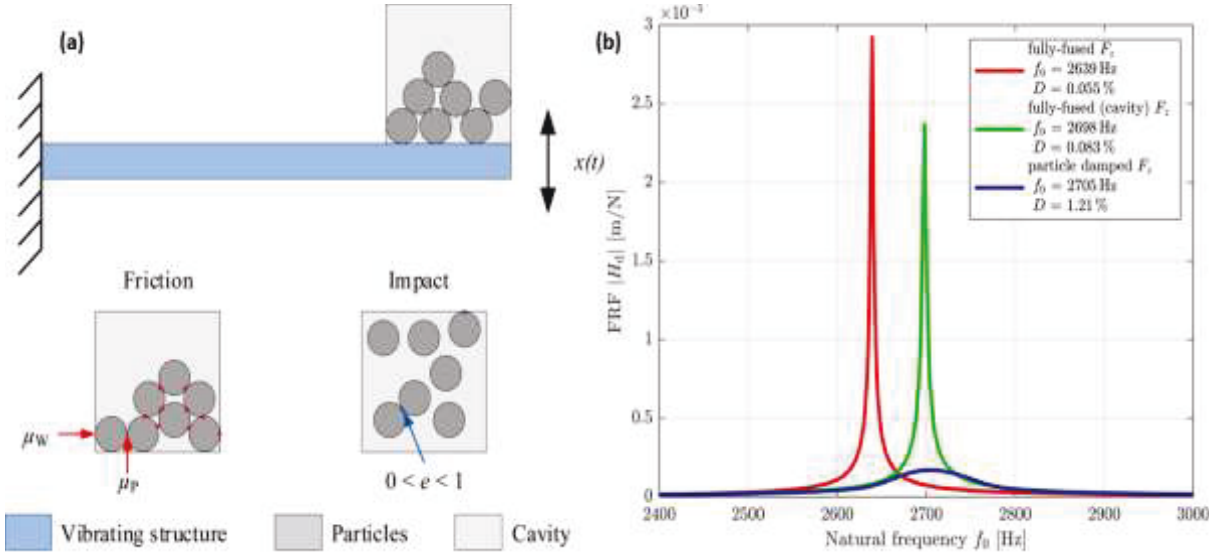

Figure 15. (a) Schematic representation of the particle damping and (b) comparative FRF response between a fully fused (with and without cavities) and a particle-damped beam (Reproduced with permission from. [113] Copyright 2022, Elsevier)

Guo et al. presented a numerical and experimental study on different structures for particle damping of AM materials.[18] The particle damping phenomenon observed in the study involves non-elastic collisions and friction, which assist in dissipating vibrational energy and thereby enable particle damping of AM materials. The experimental setup considered a cantilever beam with a particle damper attached at the beam end. This study distinguishes itself from previous research by exploring various arrangements of unfused particles within cell structures. These cells range in quantity from a single hollow cube to a box containing 64 cells within a single cube. The study also contains detailed mathematical modeling of the particle cube damper. The model assumes the cantilever beam as a Euler-Bernoulli beam for a single-degree-of-freedom system under ideal conditions,

$$M\ddot{u}(t) + C\dot{u}(t) + Ku(t) = Fp(t) \qquad \text{Equation (4)}$$

where M, C, and K are the mass, damping constant, and stiffness, respectively, and u denotes the displacement, a dot is the time derivative, and t is time. $F_p(t)$ is the impact force between the particles and walls applying on the cube. The model uses a term called specific damping capacity (SDC), which can be calculated from the ratio of kinetic energy converted to dissipative energy, either heat or sound (ΔT), to the maximum kinetic energy during a cycle (T). [18] The equation is written as follows:

$$\psi\,(SDC) = \frac{\Delta T}{T} \qquad \text{Equation (5)}$$

Figure 16 (a) provides valuable insights as the model exhibits results that are comparable to the experimental study, demonstrating the potential of mathematical models for AM materials in predicting their properties. Numerical models based on multi-physics modeling for AM materials contribute to a deeper understanding of their behavior. Furthermore, the effectiveness of utilizing a cellular structure with particle damping is demonstrated in **Figure 16 (b)** for four different samples. The graphs indicate that a damping sample with one or eight cells inside a cube exhibits superior damping capacity compared to samples with 27 or 64 cells. The Structural Damping Coefficient (SDC) results further highlight that the fully fused beam significantly lags behind the beams with particle damping, as energy dissipation is more efficient when particles are present inside the cube. [18]

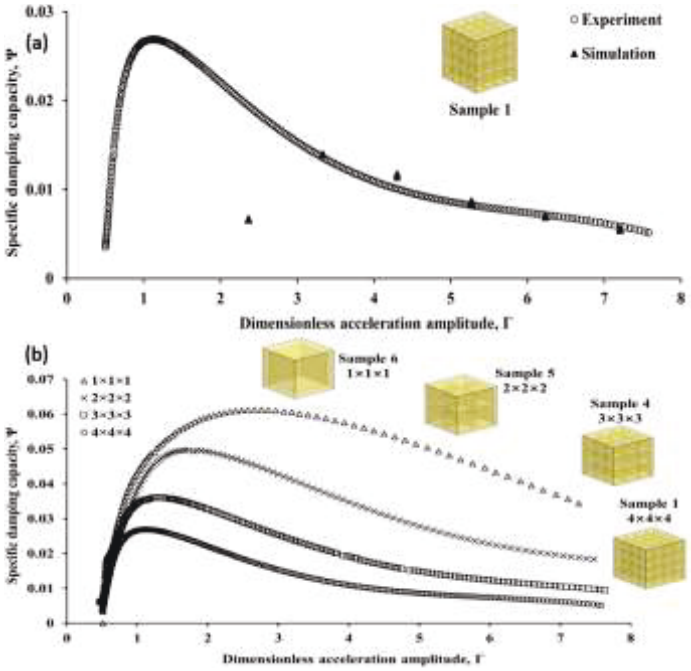

Figure 16. (a) Comparison of experimental with the simulation results at various acceleration values for a sample with 64-unit cubes inside and (b) SDC values of the samples at various acceleration values with varying sample cells inside for 1-, 8-, 27-, and 64-unit cubes inside (Reproduced with permission from. [18] Copyright 2022, Elsevier)

In their study, Onome E. et al. examined beams incorporating unfused powder and compared their damping performance with conventional fully-fused beams.[111] The findings revealed that the investigated beams could provide up to 10 times more damping than the baseline solid beam despite only a 1-4% modification of the internal beam volume. The primary mechanism for vibration suppression was identified through investigations into the impact of different parameter values on

damping. The study highlights the potential of internal feature optimization through L-PBF to enhance damping efficiency by validating the underlying physics of vibration suppression. [111]

6. Comparison of vibration analysis results between AM and conventional materials

Considering all the articles discussed above, **Table 4.** Summary of vibrational analysis of AM summarizes the AM techniques, the effect of the process parameters, printing orientation and geometry, Young's modulus, Density, natural frequency, and damping, comparing AM materials with conventionally fabricated materials. AM techniques discussed in **Table 4.** Summary of vibrational analysis of AM are SLM and LPBF, while the materials are AlSi10Mg, Inconel 718, Ti6Al4V, and some Stainless steel.

Table 4. Summary of vibrational analysis of AM

Material Fabricated	AM Techniques/ Process parameter	Printing Orientation/ Geometry	Effect on Young Modulus (E) and Density	Effect on Natural Freq./Damping as compared to the conventional fabrication process
$AlSi_{10}Mg$ [21]	SLM/ 25 µm layer thickness, 1.2 m/s scanning speed and 400 W laser power	Seven angles from 0 to 90 with three printing orientations are: Flat, Upright, Rotation	The samples printed in the Upright and Rotation orientations have a larger E value compared to the Flat and Subtractive samples	Upright and Rotation printing has the highest frequency, than flat printing. Subtractive has the least among all AM samples.
17-4 PH stainless [23]	L-PBF/ --	Horizontal (H) and Vertical (V) printing orientation	The E value of samples printed in the H direction is larger as compared to the V direction	Not discussed in the article, but a possible approach for VA for various process parameter combinations
Inconel 718 [16]	SLM/ Set of process parameters such as laser power of 120W, 140W, and 160W, scanning speed from 900mm/s, 1000mm/s and 1100mm/s and Spot size 45 µm, 60 µm,75 µm	Standard tensile specimen as per ISO 527	Spot size influences more as compared to scanning speed to change *E*. Spot size and laser power both influence more in changing the *E*. High laser power with high scanning speed also decreases the *E*	Not discussed in the article, but a possible approach for vibration analysis for various process parameter combinations
Inconel 718 [85]	L-PBF/ Five sets of process parameters such as laser power, scanning speed, and	Specimen fabrication and testing according to ASTM E8/E8M and ASTM E9	The relation established between density and process parameter set. As the Density decreases, E also decreases.	Not discussed in the article, but a possible approach for vibration analysis for various process parameter combinations

This article has been accepted for publication and undergone full peer review but has not been through the copyediting, typesetting, pagination and proofreading process, which may lead to differences between this version and the Version of Record. Please cite this article as doi: 10.1002/adem.202301650.

	hatch spacing, respectively; (i) 195W, 1.2m/s, 90 µm, (ii) 150W, 2m/s, 150 µm, (iii) 150W, 2m/s, 200 µm (iv) 100W, 2m/s, 200 µm, (v) 150W, 2m/s, 250 µm		Keeping the scanning speed and Laser power constant while increasing the hatch spacing decreases the Density and E. Keeping the scanning speed and Hatch spacing constant while decreasing the laser power decreases the Density and E.	
Stainless Steel 304L [87]	SLM/ 200W laser power, 800 mm/s scanning speed, and 50 µm layer thickness 85 and 150 µm hatch spacings.	Specimen as per ASTM E8/E8M-22 Standard Test Methods for Tension Testing of Metallic Materials	Density decreases with increases in hatch spacing and E increases till hatch spacing of 105 µm then starts to decrease. Highest value for E at hatch spacing of 105 µm	For all three modes of frequency, the frequency value increases up to 105 µm hatch spacing, then decreases with an increase in hatch spacing
Ti-6Al-4V [24]	L-PBF/ Laser power 125W, Scanning speed 2800 mm/s, Hatch spacing 110µm, Layer thickness 30µm, Laser spot diameter 60µm, Volumetric energy density 13.5 J/mm^3	Four cells with lattice structures, Cell 1 is FCCZ, Cell 2 is the rhombic dodecahedron, Cell 3 is Solidify type, Cell 4 is a stochastic type	Cells density decreases with an increase in cell unit lattice dimension. The damping ratio increases with an increase in cell unit lattice dimension (with some exceptions for cells 1 and 2 at 1.6mm). The damping ratio for all cell types at 2.4mm size is greater than a solid sample	The frequency decreases with an increase in cell unit lattice dimension. Maximum frequency obtain for cell structure Solidify type with 2.4mm, which comparable to a solid sample
Ti-6Al-4V [56]	SLM/ Laser power 75W, scanning speed 600mm/s, hatch spacing 77µm, laser beam diameter 0.11mm, and powder layer thickness 25µm	Gears used are Solid-body, Lattice structure and attice structure with a polymer insert	Lattice structured gear body lowers the maximum amplitude means better damping. Vibration reduces in gear because of the lattice structure	Frequency harmonics amplitude reduces with the incorporation of lattice structure within the gear hub

Inconel 718 [103]	SLM/ Laser power 200W, scanning speed 875mm/s, layer the thickness of 60µm, hatch spacing 90µm	Gas turbine blade similar to NACA 23012 aerofoil with the geometries that are Solid, 0.75 mm Lattice, 0.50 mm Lattice and 0.25 mm lattice	Only modal analysis was presented in the study	The solid bladehas three natural frequencies that are 1887.50, 4762.5, and 5837.50 Hz. Blade with 0.75 mm lattice has 1925.00, 4700.00, 5850.50 Hz. Blade with 0.50 mm lattice has 1962.50, 4675.00, 5900.00 Hz Blade with 0.25 mm lattice has 1987.50, 4650.00, 5950.00Hz.
$AlSi_{10}Mg$ [113]	LPBF/ Laser power of 370W, up and down skin 360W and 340W, respectively. Hatch spacing 0.19mm. Scanning speed 1300 mm/s, up and down skin 1000mm/s and 1150mm/s respectively	Fully fused beams with lying and standing positions for printing. Partially fused beams with 5%, 10%, 20% cavities	Only modal analysis was presented in the study	The natural frequency of vertical beams is greater than horizontal beams while printing A higher damping ratio was observed for partially fused beams than the fully fused beams
Stainless Steel 316 L [18]	LPBF/ laser power 107W, scanning speed of 300mm/s, line thickness of 40µm, layer thickness 25 µm, beam diameter 40µm.	Samples in cube shape comprises 1, 2, 3, and 4 small units inside it Additively Manufactured Multi-Unit Particle Damper (AM-MUPD)	Only modal analysis was presented in the study	Damping Capacity increases and then decreases for different inputs but is greater than the fully fused block. Damping capacity decreases with increases in the quantity of unit particle damper

7. Future Directions and Challenges

7.1 Limitations and challenges of existing vibration analysis techniques for AM materials

Developing specific application materials and structures like FGM using AM remains a challenging endeavor. There is a persistent limitation in thoroughly investigating the vibrational behavior of the AM parts. [7] This gap in understanding was highlighted in a study by Tevet et al., which explored the anisotropy of Ti6Al4V parts fabricated by AM in comparison to conventional methods.[114] Interestingly, the study revealed only minimal differences in elastic characteristics across various orientations. It is crucial for designers to consider the variation in elastic characteristics resulting from different manufacturing techniques and directions (i.e., AM build direction), because it can significantly affect the vibration response of the built parts. Limited research has been carried out on analyzing the effect of machining parameters on residual stresses and dynamic response during material machining operations [115], whereas the vibration characteristics of AM-manufactured parts differ from those of conventionally fabricated parts. These differences and possible challenges should also be further investigated and understood before generating models for vibration prediction. As a result, it is imperative to delve deeper into the limitations and practical challenges researchers may encounter while analyzing the vibration behavior of the AM materials. At the same time, these challenges are pivotal in shaping the future trajectory of vibrational analysis in the realm of AM. The following are the challenges and practical difficulties researchers might encounter while conducting such studies:

- *Anisotropy and Directional Dependencies:* Unlike conventionally manufactured materials, the mechanical characteristics of AM materials can vary significantly based on the build direction and orientation. Researchers may encounter practical difficulties in addressing this anisotropy, as the AM build direction introduces unique considerations for vibrational analysis. Understanding the nuanced relationship between vibrational behavior and building orientation remains a complex task.
- *Lack of Standardization in Testing Protocols:* A notable challenge in the vibrational analysis of AM materials is the lack of standardized testing protocols. Researchers often face difficulties establishing universally accepted methodologies for conducting

This article has been accepted for publication and undergone full peer review but has not been through the copyediting, typesetting, pagination and proofreading process, which may lead to differences between this version and the Version of Record. Please cite this article as doi: 10.1002/adem.202301650.

vibrational analyses on AM components, leading to variations in testing procedures and making it difficult to compare results across different studies or implement consistent quality control measures.

- *Sensitivity to Process Parameters:* AM processes are highly sensitive to a myriad of parameters, such as laser power, scanning speed, and layer thickness. These variables directly influence the mechanical properties of the final product, affecting its vibrational characteristics. Researchers may encounter practical difficulties in isolating the impact of each parameter on vibrational behavior, especially when dealing with complex geometries or intricate lattice structures.
- *Post-Processing Effects:* Most AM components undergo post-processing treatments, such as heat treatment or machining, to enhance their mechanical properties and surface finish. Understanding how these post-processing steps affect vibrational characteristics is a challenge. The interactions between the AM process and subsequent treatments pose practical difficulties in predicting the vibrational behavior of components after post-processing, requiring a comprehensive investigation into the combined effects.
- *Validation of Numerical Models:* Numerical models play a crucial role in predicting vibrational characteristics. However, validating these models for AM materials presents a unique set of challenges. Researchers must grapple with the need for extensive experimental data to verify the accuracy of numerical predictions. The inherent variability in AM material properties and the dynamic nature of the printing process further complicate the validation process.

Mitigating these challenges requires a concerted effort from the research community. Researchers should collaborate to establish standardized testing procedures, develop robust numerical models, and explore innovative approaches to account for anisotropy and sensitivity to process parameters. Emphasizing the need for transparency in reporting methodologies and results can facilitate a more systematic progression in the field of vibrational analysis for AM materials.

Moreover, understanding the physical mechanisms responsible for vibrations in AM materials is crucial. The vibrations in AM materials can result from various factors involved in the AM process. The intricate interplay of melting and solidification dynamics during the AM process primarily contributes to vibrations. As the energy from the laser or electron beam is absorbed, a rapid phase transition in the powder bed takes place and introduces thermal stresses and gradients, generating internal forces within the material. This phenomenon keeps repeating

as the material undergoes successive layers of deposition; thus, the uneven distribution of heat can give rise to transient vibrations. The localized cooling and solidification of each layer introduce variations in microstructure and material properties. These variations, in turn, create internal stresses that may manifest as vibrations during subsequent stages of the manufacturing process or during the service life of the component. As mentioned earlier, the quality of interlayer bonding and the presence of porosity contribute significantly to vibrational characteristics. Insufficient bonding between successive layers or the existence of voids and pores within the material can amplify vibrations, wherein the structural imperfections may alter the dynamic response of the material, affecting its natural frequencies and damping properties. Investigating the correlation between interlayer bonding quality, porosity, and vibrations is essential for enhancing the overall integrity of AM components. The sensitivity of AM materials to process parameters such as laser power, scanning speed, hatch space, and layer thickness plays a pivotal role in vibration generation. Variations in these parameters directly influence the energy input and cooling rates, thereby affecting the thermal history of the material and, consequently, its vibrational behavior. Understanding the intricate relationship between process parameters and vibrations is essential for optimizing the AM process and minimizing unwanted dynamic effects. In addition, adopting lattice structures and complex geometries in AM components introduces additional complexities in vibrational behavior. The intricate lattice formations, designed for lightweight and improved mechanical properties, interact with external forces, leading to vibrations. Understanding how these lattice structures respond to dynamic loads and external stimuli is crucial for predicting and managing vibrations in components with complex geometries. In summary, addressing these root causes requires tailored strategies, including optimized printing parameters, adopting controlled cooling strategies, post-processing techniques, leveraging advanced modeling techniques, refining the design of parts (e.g., lattice structures), and material design considerations are avenues to explore for minimizing vibrational issues in AM materials.

7.2. Practical Implications and Real-World Applications

The knowledge from the comprehensive review on vibrational analysis of materials manufactured through AM processes holds significant practical implications for various real-world scenarios. By understanding the vibrational characteristics of AM materials, researchers and industrial practitioners can pave the way for advancements and applications in several key areas:

- *Quality Assurance in AM:* Understanding the relationship between AM process parameters and vibrational characteristics enables better control and monitoring of the manufacturing process. Consequently, it facilitates identifying and mitigating defects such as porosity and cracks, ensuring the production of high-quality components.
- *Optimal Design of AM Components:* The vibrational analysis results provide valuable information for the optimal design of AM components. By considering the effects of geometry, process parameters, and material properties on vibrational behavior, engineers and designers can make informed decisions to enhance the structural integrity and performance of AM parts, especially in industries where lightweight and structurally efficient components are of paramount importance.
- *Development of Standard Specifications for AM Materials:* The review findings contribute to establishing standard specifications for AM materials. It involves the identification of key parameters influencing vibrational characteristics and the development of standardized testing procedures. These standards can serve as a reference for researchers and industry practitioners, fostering consistency and reliability in assessing AM materials.
- *Advancements in Predictive Maintenance:* Understanding the vibrational characteristics of AM components can be leveraged for predictive maintenance strategies. Monitoring changes in vibrational behavior allows for early detection of potential issues, reducing the risk of unexpected failures, specifically for industries where the reliability of components is critical, such as aerospace and automotive applications.

7.3. Future Research Paths

Prior research on AM parts has demonstrated that different AM techniques and post-AM heat treatment produce varying microstructures and machining behavior compared to traditional manufacturing. Given the complexity, few studies have developed Process-Structure-Property (PSP) relations through physic-based,[116–118] or data-driven models.[119–122] AM has a greater capacity to make components with complicated geometries, more operational flexibility, and shorter production times than traditional processes. However, severe problems related to the mechanical properties and surface quality of AM processes also exist. Therefore, various post-processing technologies, such as heat treatment and machining, are being used to enhance the surface quality of the parts produced through AM.[123–128] The effects of these post-processes on the vibration performance of the printed parts also need to be studied. Considering

the effect of post-processing presented in the literature on the mechanical properties of AM materials, it is critical to analyze the vibrational characteristics of materials after post-processing.[107]

Multiple modeling efforts have focused on predicting process-induced temperatures and thermal gradients in forecasting location-dependent mechanical characteristics of components. Critical temperature ranges, basic thermal frequencies, and other essential mechanistic elements of the AM process may be revealed by the framework of multi-resolution analysis and importance analysis.[129–131] The outcomes show that the developed technique can make reasonable predictions with a minimal quantity of noisy experimental data. It offers a firm foundation for a ground-breaking technique that uses cutting-edge algorithms, domain-specific knowledge, and predictions of mechanical characteristics of spatial and temporal development.[131]

Furthermore, in charting the future research paths for investigating vibrational characteristics in AM materials, it is essential to outline comprehensive methodologies encompassing experimental setups and numerical simulations. Integrating diverse approaches will facilitate a holistic understanding of the dynamic behavior of AM materials and pave the way for effective solutions to the identified challenges. Implementing advanced in-situ monitoring techniques offers an avenue for real-time observation of the AM process. High-speed cameras, thermal imaging, and acoustic emission sensors can capture dynamic events during material deposition. Integrating these technologies into the experimental setup provides valuable insights into the temporal evolution of vibrations and their correlation with specific process parameters. Conducting modal analysis and dynamic testing on fabricated components allows for directly measuring natural frequencies, damping ratios, and mode shapes. Experimental setups employing accelerometers, strain gauges, and other sensing devices facilitate the characterization of vibrational behavior under varying conditions. Excitation through controlled loading or external stimuli aids in quantifying the response of AM materials to dynamic forces. Exploring the vibrational characteristics of AM materials after post-processing treatments is a crucial aspect of experimental investigations. Heat treatment, machining, or surface finishing may influence the dynamic response of the material. Experimental setups focused on evaluating the impact of post-processing steps on vibrational properties contribute to a comprehensive understanding of the material behavior beyond the AM stage.

Additionally, leveraging numerical simulations such as Finite Element Analysis allows researchers to create virtual models of AM components and simulate their dynamic response.

Incorporating material properties, process parameters, and microstructural features into Finite Element Analysis models enables the prediction of natural frequencies and mode shapes. Sensitivity analyses within the numerical framework aid in identifying critical factors influencing vibrational behavior. One step further could be adopting multiscale modeling approaches to accommodate the hierarchical nature of AM materials, encompassing microstructural, mesoscopic, and macroscopic levels. Coupling computational tools with experimental data facilitates the development of accurate and predictive models. The integration of multiscale simulations elucidates the intricate interactions between microstructural variations and vibrational responses.

In addition to these techniques, machine learning techniques hold promise for predicting vibrational characteristics based on large datasets. Establishing correlations between process parameters, material properties, and vibrational outcomes through machine learning models enhances the predictive capabilities of numerical simulations. Such an approach can streamline the identification of optimal process conditions for desired vibrational performance. In a greater sense, machine learning algorithms can play a pivotal role in predicting material properties, optimizing process parameters, design of novel materials through identifying patterns and correlations between material compositions and vibrational behavior, using previous designs and their vibrational response to establish a feedback loop for iterative design of new structures with desirable vibration characteristics, and detection of anomalies indicating defects such as porosity or structural inconsistencies through analysis of vibrational signatures and other relevant parameters (see Figure 17 showing a general perspective of machine learning usage in enhancing the AM process). Apart from the suggested solutions, the AM community needs to develop quality assurance techniques for robust and fast certification of AM parts.

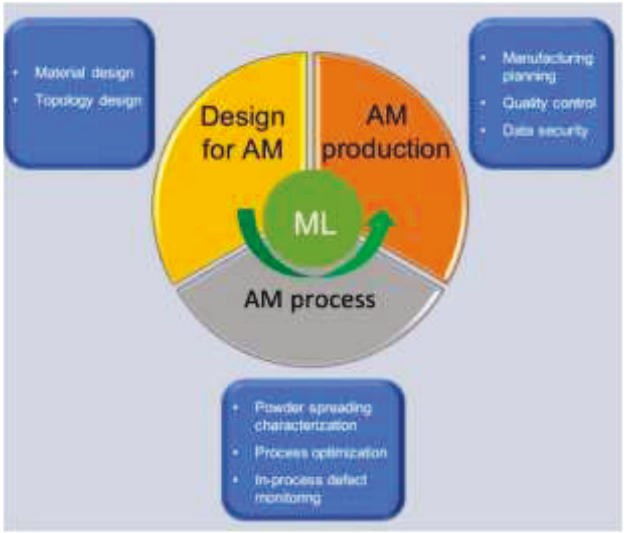

Figure 17. Possible usage of Machine Learning for design AM materials (Reproduced with permission from.[132] Copyright 2020, Elsevier)

8. Conclusions

This review discussed the vibration analysis of materials manufactured through AM, the relationship between AM process parameters and other factors, and the techniques and methods used by the author for vibrational characteristics, including experimental and simulation results. The following conclusions can be drawn:

- During the AM process, parameters such as laser power, scanning speed, spot size, etc., can significantly change the mechanical behavior of materials. Combining these process parameters changes the energy density during the process; hence, the final part property also changes. For vibration analysis, Young's modulus and Density are vital properties of the material, as the natural frequency of the fabricated part would change with both values.
- Vibration analysis effectively detects and characterizes various defects in metal alloys commonly used in AM, such as porosity, cracks, and inclusions. A solid relationship exists between AM material process parameters and vibrational characteristics. The geometry of the AM materials can also play a significant role in suppressing untoward vibrations.
- The limitations of vibration analysis for exact defect detection and characterization, such as the dependence on material properties and the need for extensive signal processing, should also be considered. Conventional numerical methods also need to be changed according to material behaviors.

- More research should be done on the finding of Young's modulus and Density as a function of AM parameters, leading to an empirical formula of the vibration relation of conventionally produced and AM materials.
- Further research is needed to address these challenges and to fully understand the potential of vibration analysis for quality control in AM. The latest techniques in this field, such as Machine and Deep Learning models, would be very effective in predicting the dynamic behavior of the AM parts.

Overall, the findings of this review highlight the importance of non-destructive testing techniques for ensuring the quality and reliability of AM parts. Furthermore, using vibration analysis and other testing methods can provide a comprehensive and efficient approach to quality control in AM.

Funding

This work has received funding from the European Union's Horizon 2020 research and innovation program under the Marie Skłodowska-Curie grant agreement No 101034425 for the project titled A2M2TECH. This study has also received funding from The Scientific and Technological Research Council of Türkiye (TUBITAK) with grant No 120C158 for the same A2M2TECH project under the TUBITAK's 2236/B program.

Received: ((will be filled in by the editorial staff))
Revised: ((will be filled in by the editorial staff))
Published online: ((will be filled in by the editorial staff))

References

[1] M. Shah, A. Ullah, K. Azher, A. U. Rehman, W. Juan, N. Aktürk, C. S. Tüfekci, M. U. Salamci, *RSC Adv.* **2023**, *13*, 1456.

[2] H. Nguyen-Xuan, K. Q. Tran, C. H. Thai, J. Lee, *Compos. Struct.* **2023**, *315*, 116981.

[3] I. Gibson, D. Rosen, B. Stucker, M. Khorasani, *Addit. Manuf. Technol.* **2021**.

[4] A. Bandyopadhyay, S. Bose, *Additive manufacturing*, **2019**.

[5] M. Shah, A. Ullah, K. Azher, A. Ur Rehman, N. Akturk, W. Juan, C. S. Tüfekci, M. U. Salamci, *Cryst. 2023, Vol. 13, Page 285* **2023**, *13*, 285.

[6] S. A. M. Tofail, E. P. Koumoulos, A. Bandyopadhyay, S. Bose, L. O'Donoghue, C. Charitidis, *Mater. Today* **2018**, *21*, 22.

[7] L. Yan, Y. Chen, F. Liou, *Addit. Manuf.* **2020**, *31*, 100901.

[8] M. Biyikli, T. Karagoz, M. Calli, T. Muslim, A. A. Ozalp, A. Bayram, *Met. Mater. Int.* **2023**, *29*, 807.

[9] İ. Aktitiz, R. Varol, N. Akkurt, M. F. Saraç, *Polym. Test.* **2020**, *90*, 106724.

[10] M. A. Mahmood, A. U. Rehman, F. Pitir, M. U. Salamci, I. N. Mihailescu, *Materials (Basel).* **2021**, *14*.

[11] S. Zhao, K. Yuan, W. Guo, Y. He, Y. Xu, X. Lin, *Int. J. Fatigue* **2020**, *136*, 105629.

[12] T. Duda, L. V. Raghavan, *IFAC-PapersOnLine* **2016**, *49*, 103.

[13] R. Ranjan, D. Kumar, M. Kundu, S. Chandra Moi, *Mater. Today Proc.* **2022**, *61*, 43.

[14] M. A. Mahmood, A. Ullah, M. Shah, A. U. Rehman, M. U. Salamci, M. Khraisheh, *Handb. Post-Process. Addit. Manuf. Requir. Theor. Methods* **2023**, 87.

[15] P. Ponnusamy, R. A. R. Rashid, S. H. Masood, D. Ruan, S. Palanisamy, *Materials (Basel).* **2020**, *13*, 4301.

[16] N. Kladovasilakis, P. Charalampous, K. Tsongas, I. Kostavelis, D. Tzovaras, D. Tzetzis, *Materials (Basel).* **2022**, *15*, 1.

[17] G. R. Cobb, A. J. Lingenfelter, A. D. C. Nesmith, R. P. O'Hara, *AIAA/ASCE/AHS/ASC Struct. Struct. Dyn. Mater. Conf. 2018* **2018**.

[18] H. Guo, K. Ichikawa, H. Sakai, H. Zhang, X. Zhang, K. Tsuruta, K. Makihara, A. Takezawa, *Powder Technol.* **2022**, *396*, 696.

[19] S. Ehsan Saghaian, M. Nematollahi, G. Toker, A. Hinojos, N. Shayesteh Moghaddam, S. Saedi, C. Y. Lu, M. Javad Mahtabi, M. J. Mills, M. Elahinia, H. E. Karaca, *Opt. Laser Technol.* **2022**, *149*, 107680.

[20] C. Phutela, F. Bosio, A. Alhammadi, N. Alshehhi, L. Kindleyside, N. T. Aboulkhair,

Z. Guan, C. Phutela, F. Bosio, A. Alhammadi, N. Alshehhi, L. Kindleyside, N. T. Aboulkhair, *Metals (Basel).* **2023**, *13*, 151.

[21] P. Lesage, L. Dembinski, R. Lachat, S. Roth, *Results Eng.* **2022**, *13*.

[22] P. Hartunian, M. Eshraghi, *J. Manuf. Mater. Process.* **2018**, *2*, 69.

[23] H. Ghadimi, A. P. Jirandehi, S. Nemati, H. Ding, A. Garbie, J. Raush, C. Zeng, S. Guo, *Materials (Basel).* **2023**, *16*.

[24] J. Liu, K. Guo, J. Sun, Q. Sun, L. Wang, H. Li, *J. Manuf. Process.* **2021**, *66*, 1.

[25] D. Wang, C. Song, Y. Yang, Y. Bai, *Mater. Des.* **2016**, *100*, 291.

[26] J. Hajnys, M. Pagac, O. Kotera, J. Petru, S. Scholz, *MM Sci. J.* **2019**, *2019*, 2790.

[27] Z. F. Fu, J. He, *Modal Analysis*, Elsevier Science, **2001**.

[28] P. D. Ravi, D. Seshu, *ASIAN J. Civ. Eng. (BUILDING HOUSING)* **2008**.

[29] A. Harake, *Master's Theses* **2022**.

[30] L. O. B. Coronado, L. I. M. Ballesteros, E. J. T. Geraldo, A. M. Buison, U. B. Ante, J. B. L. Padaca, V. Sarmiento, D. D. A. Florante, J. A. V. Garcia, F. P. Liza, *2021 IEEE 13th Int. Conf. Humanoid, Nanotechnology, Inf. Technol. Commun. Control. Environ. Manag. HNICEM* **2021**.

[31] A. Arjunan, A. Baroutaji, A. S. Praveen, A. G. Olabi, C. J. Wang, *Ref. Modul. Mater. Sci. Mater. Eng.* **2019**.

[32] A. Arjunan, A. Baroutaji, A. Latif, *Results Eng.* **2021**, *11*, 100252.

[33] C. Galy, E. Le Guen, E. Lacoste, C. Arvieu, *Addit. Manuf.* **2018**, *22*, 165.

[34] B. Zhang, Y. Li, Q. Bai, *Chinese J. Mech. Eng.* **2017**, *30*, 515.

[35] Z. W. Xu, Q. Wang, X. S. Wang, C. H. Tan, M. H. Guo, P. B. Gao, *Mech. Mater.* **2020**, *148*, 103499.

[36] P. Yadav, O. Rigo, C. Arvieu, E. Le Guen, E. Lacoste, *Crystals* **2020**, *10*, 524.

[37] D. Y. Pimenov, L. F. Berti, G. Pintaude, G. X. Peres, Y. Chaurasia, N. Khanna, K.

Giasin, *Int. J. Adv. Manuf. Technol.* **2023**, *127*, 1071.

[38] T. Voisin, N. P. Calta, S. A. Khairallah, J. B. Forien, L. Balogh, R. W. Cunningham, A. D. Rollett, Y. M. Wang, *Mater. Des.* **2018**, *158*, 113.

[39] G. Kalusuraman, S. T. Kumaran, K. Balamurugan, N. Sivashanmugam, P. Sivaprakasam, R. Kurniawan, V. Ezhilmaran, *J. Nat. Fibers* **2023**, *20*, 2157361.

[40] Z. Murčinková, P. Adamčík, D. Sabol, *Polymers (Basel).* **2022**, *14*.

[41] S. K. Georgantzinos, G. I. Giannopoulos, S. I. Markolefas, *Materials (Basel).* **2020**, *13*, 4225.

[42] N. D. Tilahun, H. G. Lemu, *Lect. Notes Inst. Comput. Sci. Soc. Telecommun. Eng. LNICST* **2021**, *385*, 357.

[43] Z. K. Peng, Z. Q. Lang, S. A. Billings, Y. Lu, *Int. J. Mech. Sci.* **2007**, *49*, 1213.

[44] P. Sengsri, S. Kaewunruen, *Mater. Today Proc.* **2022**, *65*, 1656.

[45] Y. Chen, A. Linderholt, T. Abrahamsson, *Conf. Proc. Soc. Exp. Mech. Ser.* **2014**, *2*, 35.

[46] M. L. Chandravanshi, A. K. Mukhopadhyay, *ASME Int. Mech. Eng. Congr. Expo. Proc.* **2014**, *14*.

[47] Q. Guo, Y. Liu, B. Chen, Y. Zhang, *Ocean Eng.* **2021**, *237*, 109630.

[48] Q. Guo, Y. Liu, B. Chen, Y. Zhao, *Eur. J. Mech. - A/Solids* **2021**, *86*, 104155.

[49] X. Liu, W. Sun, X. Yan, D. Du, H. Liu, H. Li, *Thin-Walled Struct.* **2023**, *183*, 110369.

[50] E. Sobhani, M. Koohestani, Ö. Civalek, M. Avcar, *Eng. Anal. Bound. Elem.* **2023**, *149*, 38.

[51] F. Pashmforoush, *Proc. Inst. Mech. Eng. Part C J. Mech. Eng. Sci.* **2022**, *237*, 782.

[52] P. Sharma, M. Gautam, M. Chaturvedi, *Mater. Today Proc.* **2022**, *62*, 4222.

[53] P. Sharma, B. Gupta, S. K. Rathore, *Mater. Today Proc.* **2022**, *62*, 3647.

[54] A. Koyuncu, T. Karaağaçlı, M. Şahin, H. N. Özgüven, *Exp. Mech.* **2022**, *62*, 1579.

[55] S. Yin, T. Yu, T. Q. Bui, P. Liu, S. Hirose, *Comput. Struct.* **2016**, *177*, 23.

[56] R. Ramadani, S. Pal, M. Kegl, J. Predan, I. Drstvenšek, S. Pehan, A. Belšak, *Int. J. Adv. Manuf. Technol.* **2021**, *113*, 3389.

[57] M. J. K. Lodhi, K. M. Deen, M. C. Greenlee-Wacker, W. Haider, *Addit. Manuf.* **2019**, *27*, 8.

[58] J. A. Tamayo, M. Riascos, C. A. Vargas, L. M. Baena, *Heliyon* **2021**, *7*, e06892.

[59] P. Platek, J. Sienkiewicz, J. Janiszewski, F. Jiang, *Materials (Basel).* **2020**, *13*, 2204.

[60] L. H. Olivas-Alanis, A. A. Fraga-Martínez, E. García-López, O. Lopez-Botello, E. Vazquez-Lepe, E. Cuan-Urquizo, C. A. Rodriguez, *Materials (Basel).* **2023**, *16*, 1025.

[61] N. Sundararajan, T. Prakash, M. Ganapathi, *Finite Elem. Anal. Des.* **2005**, *42*, 152.

[62] Z. hai Wang, X. hong Wang, G. dong Xu, S. Cheng, T. Zeng, *Compos. Struct.* **2016**, *135*, 191.

[63] V. Kahya, M. Turan, *Compos. Part B Eng.* **2018**, *146*, 198.

[64] M. Talha, B. N. Singh, *Finite Elem. Anal. Des.* **2011**, *47*, 394.

[65] J. Da Cunha Vaz, J. J. De Lima Junior, *JVC/Journal Vib. Control* **2016**, *22*, 193.

[66] S. S. Rao, P. Griffin, *Mechanical vibrations*, 6th ed., **2017**.

[67] F. W. Williams, W. H. Wittrick, *Int. J. Mech. Sci.* **1970**, *12*, 781.

[68] L. Bellagamba, T. Y. Yang, *AIAA J.* **2012**, *19*, 1452.

[69] A. Siddika, M. R. Awall, M. A. Al Mamun, T. Humyra, *Comput. Eng. Phys. Model.* **2019**, *2*, 36.

[70] B. ELLIS, BRE, *Proc. Inst. Civ. Eng.* **1980**, *69*, 763.

[71] J. P. Kruth, L. Froyen, J. Van Vaerenbergh, P. Mercelis, M. Rombouts, B. Lauwers, *J. Mater. Process. Technol.* **2004**, *149*, 616.

[72] M. Shiomi, A. Yoshidome, F. Abe, K. Osakada, *Int. J. Mach. Tools Manuf.* **1999**, *39*, 237.

[73] R. Rai, J. W. Elmer, T. A. Palmer, T. Debroy, *J. Phys. D. Appl. Phys.* **2007**, *40*, 5753.

[74] D. B. Hann, J. Iammi, J. Folkes, *J. Phys. D. Appl. Phys.* **2011**, *44*, 445401.

[75] H. Ghadimi, A. P. Jirandehi, S. Nemati, S. Guo, *Fatigue Fract. Eng. Mater. Struct.* **2021**, *44*, 3517.

[76] S. Z. Hussain, Z. Kausar, Z. U. Koreshi, S. R. Sheikh, H. Z. U. Rehman, H. Yaqoob, M. F. Shah, A. Abdullah, F. Sher, *Processes* **2021**, *9*, 1547.

[77] Y. Wang, L. Zheng, Y. Gao, S. Li, *IEEE Access* **2020**, *8*, 224092.

[78] S. Z. Hussain, Z. Kausar, Z. U. Koreshi, S. R. Sheikh, H. Z. U. Rehman, H. Yaqoob, M. F. Shah, A. Abdullah, F. Sher, *Process. 2021, Vol. 9, Page 1547* **2021**, *9*, 1547.

[79] Damping in Structural Dynamics: Theory and Sources, **2019**.

[80] J. J. Andrew, J. Schneider, J. Ubaid, R. Velmurugan, N. K. Gupta, S. Kumar, *Int. J. Impact Eng.* **2021**, *149*, 103768.

[81] P. Hanzl, M. Zetek, T. Bakša, T. Kroupa, *Procedia Eng.* **2015**, *100*, 1405.

[82] K. S. Jeong, C. Y. Kang, *Korean J. Mater. Res.* **2016**, *26*, 493.

[83] J. H. Kim, M. S. Lee, J. S. Kim, *Materials (Basel).* **2021**, *14*, 7160.

[84] K. Guan, Z. Wang, M. Gao, X. Li, X. Zeng, *Mater. Des.* **2013**, *50*, 581.

[85] M. Valdez, C. Kozuch, E. J. Faierson, I. Jasiuk, *J. Alloys Compd.* **2017**, *725*, 757.

[86] X. Yan, J. Pang, Y. Jing, *Materials (Basel).* **2019**, *12*, 2719.

[87] B. M. West, N. E. Capps, J. S. Urban, J. D. Pribe, T. J. Hartwig, T. D. Lunn, B. Brown, D. A. Bristow, R. G. Landers, E. C. Kinzel, *Manuf. Lett.* **2017**, *13*, 30.

[88] V. Giurgiutiu, *Stress, Vibration, and Wave Analysis in Aerospace Composites: For SHM and NDE Applications*, Elsevier, **2022**.

[89] S. Braun, D. Ewins, S. Rao, *Encyclopedia of vibration*, **2002**.

[90] R. Rashid, S. H. Masood, D. Ruan, S. Palanisamy, R. A. Rahman Rashid, J. Elambasseril, M. Brandt, *Addit. Manuf.* **2018**, *22*, 426.

[91] R. Harkin, H. Wu, S. Nikam, S. Yin, R. Lupoi, P. Walls, W. McKay, S. McFadden, *Int. J. Adv. Manuf. Technol.* **2023**, *126*, 659.

[92] P. Ferro, R. Meneghello, G. Savio, F. Berto, *Int. J. Adv. Manuf. Technol.* **2020**, *110*, 1911.

[93] R. Zhao, C. Chen, W. Wang, T. Cao, S. Shuai, S. Xu, T. Hu, H. Liao, J. Wang, Z. Ren, *Addit. Manuf.* **2022**, *51*, 102605.

[94] L. Dowling, J. Kennedy, D. Trimble, *J. Manuf. Process.* **2022**, *77*, 607.

[95] K. Bari, A. Arjunan, *J. Mech. Behav. Biomed. Mater.* **2019**, *95*, 1.

[96] S. P. Yadav, R. S. Pawade, *Metals (Basel).* **2023**, *13*.

[97] Y. Zhang, S. Bai, M. Riede, E. Garratt, A. Roch, *Addit. Manuf.* **2020**, *34*, 101256.

[98] C. Yan, L. Hao, A. Hussein, S. L. Bubb, P. Young, D. Raymont, *J. Mater. Process. Tech.* **2014**, *4*, 856.

[99] C. Cosma, I. Drstvensek, P. Berce, S. Prunean, S. Legutko, C. Popa, N. Balc, *Materials (Basel).* **2020**, *13*, 4123.

[100] T. Maconachie, M. Leary, B. Lozanovski, X. Zhang, M. Qian, O. Faruque, M. Brandt, *Mater. Des.* **2019**, *183*, 108137.

[101] G. Kelly, *Mechnical Vibrations Theory and Applications*, Cengage Learning, **2006**.

[102] M. Kam, H. Saruhan, A. İpekçi, *J. Thermoplast. Compos. Mater.* **2022**, *36*, 2505.

[103] S. Hussain, W. A. W. Ghopa, S. S. K. Singh, A. H. Azman, S. Abdullah, *Metals (Basel).* **2022**, *12*, 340.

[104] A. Presas, D. Valentin, C. Valero, M. Egusquiza, E. Egusquiza, *Appl. Sci.* **2019**, *9*, 3864.

[105] U. Simsek, A. Akbulut, C. E. Gayir, C. Basaran, P. Sendur, *Int. J. Adv. Manuf. Technol.* **2021**, *115*, 657.

[106] K. Bari, L. Bollenbach, *J. Compos. Sci.* **2022**, *6*.

[107] J. Raval, A. Kazi, O. Randolph, X. Guo, R. Zvanut, C. Lee, B. Tai, *J. Manuf. Process.* **2023**, *94*, 539.

[108] O. Scott-Emuakpor, L. Sheridan, B. Runyon, T. George, *J. Eng. Gas Turbines Power* **2021**, *143*.

[109] O. Scott-Emuakpor, A. Schoening, A. Goldin, J. Beck, B. Runyon, T. George, *AIAA Scitech 2021 Forum* **2021**, *59*, 379.

[110] O. Scott-Emuakpor, T. George, B. Runyon, C. Holycross, B. Langley, L. Sheridan, R. O'Hara, P. Johnson, J. Beck, In *ASME Turbo Expo 2018: Turbomachinery Technical Conference and Exposition*, American Society of Mechanical Engineers Digital Collection, **2018**.

[111] O. Scott-Emuakpor, T. George, B. Runyon, J. Beck, L. Sheridan, C. Holycross, R. O'hara, *AIAA Scitech 2019 Forum* **2019**.

[112] M. Postell, D. Kiracofe, O. Scott-Emuakpor, T. George, *Conf. Proc. Soc. Exp. Mech. Ser.* **2023**, 87.

[113] T. Ehlers, S. Tatzko, J. Wallaschek, R. Lachmayer, *Addit. Manuf.* **2021**, *38*, 101752.

[114] O. Tevet, D. Svetlizky, D. Harel, Z. Barkay, D. Geva, N. Eliaz, *Materials (Basel).* **2022**, *15*.

[115] P. Durai Murugan, S. Vijayananth, M. P. Natarajan, D. Jayabalakrishnan, K. Arul, V. Jayaseelan, J. Elanchezhian, *Mater. Today Proc.* **2022**, *59*, 1277.

[116] W. Yan, Y. Lian, C. Yu, O. L. Kafka, Z. Liu, W. K. Liu, G. J. Wagner, *Comput. Methods Appl. Mech. Eng.* **2018**, *339*, 184.

[117] C. Herriott, X. Li, N. Kouraytem, V. Tari, W. Tan, B. Anglin, A. D. Rollett, A. D. Spear, *Model. Simul. Mater. Sci. Eng.* **2019**, *27*, 025009.

[118] R. Shi, S. Khairallah, T. W. Heo, M. Rolchigo, J. T. McKeown, M. J. Matthews, *JOM* **2019**, *71*, 3640.

[119] L. Lu, M. Dao, P. Kumar, U. Ramamurty, G. E. Karniadakis, S. Suresh, *Proc. Natl. Acad. Sci. U. S. A.* **2020**, *117*, 7052.

[120] M. Assi, J. Favre, A. Fraczkiewicz, F. Tancret, *J. Mater. Sci. 2022 5728* **2022**, *57*, 13446.

[121] A. Raza, K. M. Deen, R. Jaafreh, K. Hamad, A. Haider, W. Haider, *Int. J. Adv. Manuf. Technol.* **2022**, *122*, 1143.

[122] R. Liu, S. Liu, X. Zhang, *Int. J. Adv. Manuf. Technol.* **2021**, *113*, 1943.

[123] X. Peng, L. Kong, J. Y. H. Fuh, H. Wang, *J. Manuf. Mater. Process. 2021, Vol. 5, Page 38* **2021**, *5*, 38.

[124] H. Tang, C. Gao, Y. Zhang, N. Zhang, C. Lei, Y. Bi, P. Tang, J. H. Rao, *J. Mater. Sci. Technol.* **2023**, *139*, 198.

[125] S. Fries, A. Vogelpoth, A. Kaletsch, C. Broeckmann, *Int. J. Refract. Met. Hard Mater.* **2023**, *111*, 106085.

[126] F. Großwendt, A. Röttger, A. Strauch, A. Chehreh, V. Uhlenwinkel, R. Fechte-Heinen, F. Walther, S. Weber, W. Theisen, *Mater. Sci. Eng. A* **2021**, *827*, 142038.

[127] E. J. Kim, C. M. Lee, D. H. Kim, *J. Mater. Res. Technol.* **2021**, *15*, 1370.

[128] T. Han, C. H. Kuo, N. Sridharan, L. M. Headings, S. S. Babu, M. J. Dapino, *Mater. Sci. Eng. A* **2020**, *769*, 138457.

[129] S. Liu, K. Lee, P. V. Balachandran, *J. Appl. Phys.* **2022**, *132*, 105105.

[130] H. L. Wei, T. Mukherjee, W. Zhang, J. S. Zuback, G. L. Knapp, A. De, T. DebRoy, *Prog. Mater. Sci.* **2021**, *116*, 100703.

[131] X. Xie, J. Bennett, S. Saha, Y. Lu, J. Cao, W. K. Liu, Z. Gan, *npj Comput. Mater.* **2021**, *7*, 1.

[132] C. Wang, X. P. Tan, S. B. Tor, C. S. Lim, *Addit. Manuf.* **2020**, *36*, 101538.

Kashif Azher

Kashif Azher received his B.E. degree in Mechanical Engineering from the NED University of Engineering and Technology, Pakistan, in (2013–2016) and his M.S. degree in Mechanical Engineering from the National Taiwan University of Science and Technology, Taiwan, in (2018–2020). Previously, he served as a Lecturer in the Mechanical Engineering Department at NED University of Engineering and Technology. He is working as a researcher on the Design for Additive Manufacturing (AM) projects. Azher's research interests include nanomaterial fabrication and characterization and structural analysis of additively manufactured parts.

Mussadiq Shah

Mussadiq Shah earned his bachelor's in Mechanical Engineering from the University of Wah, Pakistan, in 2018, and later obtained his master's. in Materials Science and Engineering from

Xian Jiaotong University, China, in 2021. As a former R&D Engineer at Polymaker in Shanghai, China, he actively contributed to the developments of innovative materials for FDM 3D printing. He possesses both industry and academia experience in multiple additive manufacturing technologies like SLA/DLP, FDM, SLM,DED etc.. Currently, his research primarily focuses on process and materials development for metal and ceramic 3D printing.

Ahmad Reshad BAKHTARI

Ahmad Reshad Bakhtari is a PhD candidate in Mechanical Engineering at Gazi University. Previously a research fellow at the Indian Institute of Science Bangalore, he currently serves as an Early-Stage Researcher at the Additive Manufacturing Technology and Research Center (EKTAM) under the A2M2Tech project. His research focuses on laser-material interaction in Additive Manufacturing. Specifically, he explores innovative laser beam scanning strategies and beam parameter interactions for net-shape Additive Manufacturing of AlSi10Mg alloys aerospace components.

Andrea Cini

Andrea Cini obtained the BSc and the MSc in Aeronautical Engineering, from the University of Pisa in 2003 and 2006 respectively and a PhD degree in Fatigue and Damage Tolerance at Cranfield University, UK, in 2009. Subsequently he developed his research activity in Aerostructures and Fatigue and Damage Tolerance as research Fellow at Cranfield University, Scuola Sant'Anna, Pisa, the University of Nottingham and as manager of the Design and Development department of the automotive company Asso Werke s.r.l. In July 2019 he joined University Carlos III of Madrid as "Profesor Visitante" where he leads the ASD Lab.

Table of content (text)

In this review paper, recent advances in the application of vibration analysis for identifying and characterizing flaws in metal alloys produced by additive manufacturing has been summarized. This paper also includes studies on defects, such as porosity, cracks, and inclusions, and their effect on vibration analysis. The article concludes with a discussion of the limitations of vibrational analysis for defect characterization and future research directions.

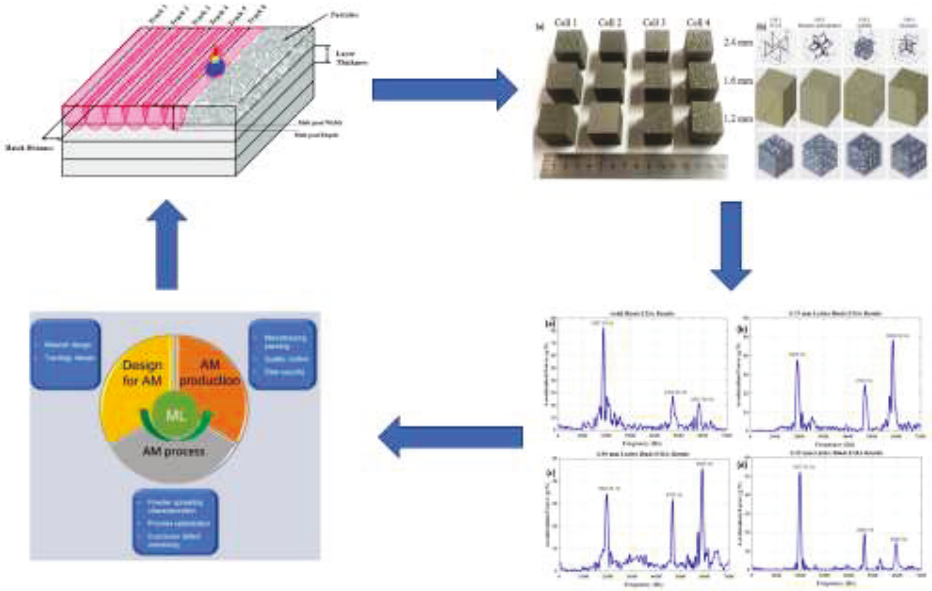

2024-01-19

A review on vibration characteristics of additively manufactured metal alloys

Azher, Kashif

Wiley

Azher K, Shah M, Bakhtari AR, et al., (2024) A review on vibration characteristics of additively manufactured metal alloys. Advanced Engineering Materials, Volume 26, Issue 6, March 2024, Article number 2301650

https://doi.org/10.1002/adem.202301650